

Bhawani Regmi

Potential of microalgae for Biofuel

An experimental study on the effects of light irradiance and photoperiod on the growth rate and lipid content in microalgae *Phaeodactylum tricornutum*

Helsinki Metropolia University of Applied Sciences

Bachelors in Engineering

Environmental Engineering

Bachelor's thesis

22.05.2014

Author	Bhawani Regmi
Title	Potential of microalgae for biofuel
Number of Pages	64 pages + 1 appendix
Date	22 May 2014
Degree	Bachelors in Engineering
Degree Programme	Environmental Engineering
Specialisation option	Water, Waste and Environmental Engineering
Instructor(s)	Jukka Seppälä, Head of the unit, Marine Research Centre, Finnish Environment Institute Docent Veli-Matti Taavitsainen, Principle lecturer Dr. Minna -Paananen-Porkka, Lecturer
<p>Microalgae appear as an alternative source of biofuel due to their oil content, metabolic flexibility, ability to grow in non-arable land and their ability to use fertilizers with 100% efficiency. To make the biodiesel production from microalgae more feasible and economical, several features of microalgae has to be studied. Illumination factors such as photoperiod and irradiance can significantly affect the growth and lipid content in microalgae. To optimize the growth and lipid content in a microalgae culture system, the effects of light irradiance and photoperiod on the growth, biomass productivity and lipid content were studied in a batch culture under controlled laboratory conditions.</p> <p>The study was divided into two discrete sets of experiments. In the first experiment, <i>P. tricornutum</i> was cultivated under four fixed irradiance levels 400, 180, 40, and 20 $\mu\text{mol}\cdot\text{q}\cdot\text{m}^{-2}\cdot\text{s}^{-1}$ at six different day lengths 4,8,12,16,20,and 24 h. The growth rate and lipid content were observed at the exponential phase. Growth rates were found to be higher at a photoperiod of 20 h at irradiance level of 400 $\mu\text{mol}\cdot\text{q}\cdot\text{m}^{-2}\cdot\text{s}^{-1}$, while the lowest were observed at a photoperiod of 4h. A phenomenon of photoinhibition was also observed at a photoperiod of 24 h. In the second experiment, two reasonably higher and lower growth rates and light levels were chosen and the species were cultivated in nutrient-depleted medium. The growth rates and variation in lipid content were studied at the stationary phase. Moreover, a lipid growth model was made in R to check the effects of light irradiance and photoperiods at the exponential and stationary phase. The lipid production was found to favor the longer photoperiod and higher irradiances only at the stationary phase.</p>	

The results obtained from this study will help in modeling and evaluating the growth of microalgae at varying light intensities and photoperiods in different locations around the globe. In addition, the results will also provide basic understanding of the production limits globally.

Keywords

microalgae, biofuel, lipids, irradiance, photoperiod

Acknowledgement

This Bachelor's thesis was carried out at the Marine Research Centre of Finnish Environment Institute as a part of SUBMARINER research project 'Potential uses of micro and macro algae in the Baltic Sea Region co-funded by the EU.

I would like to express my immense gratitude to my supervisor PhD. Jukka Seppälä for providing me this opportunity. I am indebted to him. Without his support and guidance, I wouldn't have done so much.

I would also like to thank my supervisors Docent Veli-Matti Taavitsainen, and Dr. Minna Paananen- Porkka for their support during thesis writing. I would also like to thank senior lecturer Kaj Lindedahl, Dr. Antti Tohka, Dr. Esa Toukonitty, Juha Tuomas Vuorisalo, study co-ordinator Jenni Merjankaari, Marja Lenna Åkerman and all other teachers and staffs for their valuable support during the study period. The three years in Metropolia School would not have been easier without their flexibility and assistance.

I cannot stay away without thanking my great friends Ahti, Niina, Lina and especially, Heini and family throughout their great support during my studies and for helping me to mingle in Finnish culture with so much ease. Thanks to all my friends in TG10 and TG11 in Metropolia.

I also wish to thank Katariina Natunen who helped me during the experiments and analysis at the Marine Research laboratory of SYKE. Thank you everyone at Marine laboratory of SYKE for their assistance and special coffee time together during the internship period.

Last but not the least, my father Lila Prasad Regmi, my mother Sita Regmi, my uncle Dhan Prasad, and my sister Bhawana for supporting me and making me brave enough to come to Finland. I love them and I miss them very much. This is dedicated to them.

Bhawani Regmi
Espoo, Finland

List of Table

Table 1. Common sources of biodiesel including microalgae and their oil yield.	3
Table 2. Lipid content in microalgae species	4
Table 3. Excitation emission settings for spectrofluorometer.	30
Table 4. Calculated growth rates using least square regression analysis at irradiances 400, 180, 40 and 20 $\mu\text{mol} \cdot \text{q} \cdot \text{m}^{-2} \cdot \text{s}^{-1}$ and photoperiod 4, 8, 12, 16, 20, and 24 h.	34
Table 5. Specific growth rates and growth saturation parameter values obtained from nonlinear regression in R.	37
Table 6. Rate of increase in lipids per day.	48
Table 7. Data matrix for the NR. Per DW for the model.	49

List of Figures

Figure 1. Morphology of a microalgae cell.	7
Figure 2. Five growth phases of the micro algae culture.	7
Figure 3. Factors affecting energy conversion during photosynthesis from solar irradiance to organic matter in microalgae.	9
Figure 4. Yearly sum of global irradiance averages over the period of 1981 to 2000. (Meteonorm)	10
Figure 5. World map of algae biomass productivity (tones $\text{ha}^{-1} \text{ year}^{-1}$) at 5% photosynthetic efficiency considering energy content at 20 MJ Kg^{-1} dry biomass.	11
Figure 6. Schematic diagram of open raceway algae cultivation system	15
Figure 7. A schematic diagram of a photobioreactor	16
Figure 8. Tri glycerol (neutral lipid) and phospho lipid (right).	18
Figure 9. Microscope pictures of <i>Phaeodactylum tricornutum</i> with other species (on left) and Individual cell figure (on right) by Alessandra de Martino and Chris Bowler, Stazione Zoologica and Ecole Normale Supérieure.	24
Figure 10. Instrumental set up for Experiment 1	26
Figure 11. Instrumental set up for Experiment 2	27
Figure 12. Filtration unit (a) and biomass samples on the filters (b).	31
Figure 13. Graph (a) (b) (c) (d) (e) (f) Exponential growth curve for photoperiods and 4, 8, 12, 16, 20, 24 h at irradiances each 400, 150, 40, 20 $\mu\text{mol} \cdot \text{q} \cdot \text{m}^{-2} \cdot \text{s}^{-1}$ irradiances.	34
Figure 14. Contour plot of the growth rates with respect to the irradiances and photoperiods.	36
Figure 15. Growth irradiance curve based on the observation values and fitted values (a) L-4, (b) L-8, (c) L-12, (d) L-16, (e) L-20 and (f) L-24.	39
Figure 16. Photoperiod vs. growth saturation parameter (K_e).	39
Figure 17. Photoperiod vs. specific growth rate	40

Figure 18. Chlorophyll per dry weight vs. the light dose.....	41
Figure 19. Contour plot for Chla/dry weight.....	42
Figure 20. Nile red fluorescence vs. dry weight at photo period 20 h.....	43
Figure 21. Contour plot for NR fluorescence per dry weight.	43
Figure 22. NR per Dry weight vs. the light dose.....	44
Figure 23. Growth curves at the stationary phase (a) L-20 and (b) for L-8 photoperiod.	46
Figure 24. Log of NR per day for (a) L-20 and (b) L-8.....	47
Figure 25. Rate of increase in NR per day for photoperiod 20 and 8	49
Figure 26. R output summary for Model 1 and Model 2 of lipid growth at exponential phase and stationary phase.	51
Figure 27. Contour plot of Model 2.....	52

List of Abbreviations

Chla: Chlorophyll a

NR: Nile Red

NR per DW: Nile Red per Dry weight

PAR: Photosynthetically active radiation

DMSO: Di-methyl sulfoxide

TAG: Tri-acyl glycerol

FAME: Fatty acid methyl esters

FFA: Free fatty acids

NPQ: Non photochemical quenching

OJIP: Chlorophyll fluorescence transient

LC₁: Light curve 1

LC₂: Light curve 2

L-4: Photoperiod 4h

L-8: Photoperiod 8h

L-12: Photoperiod 12h

L-16: Photoperiod 16h

L- 20: Photoperiod 20h

L-24: Photoperiod 24h

Table of Contents

1	Introduction	1
1.1	World Energy Outlook	1
1.2	Biofuel as energy feedstock	2
1.3	Microalgae as energy feedstock	2
2	Literature Review	6
2.1	Microalgae	6
2.1.1	Morphology	6
2.2	Factors affecting growth of microalgae	8
2.2.1	Light supply	8
2.2.2	Nutrients	11
2.2.3	Temperature	12
2.2.4	pH	13
2.2.5	Salinity	13
2.3	Algae cultivation principles	13
2.4	Commercial scale cultivation	14
2.4.1	Open and raceways ponds	14
2.4.2	Closed photobioreactors	15
2.5	Algae Lipids	17
3	Algae biomass harvesting techniques	19
3.1	Filtration	19
3.2	Centrifugation	20
3.3	Flocculation	20
3.4	Electrophoresis	20
4	Experimental	22
4.1	Aims of the study	22
4.2	Material and Methods	23
4.2.1	Species selection	23
4.2.2	Cultivation	25
4.2.3	LED, Light Measurements and Power Setup	25
4.2.4	Instrumental setup for Experiment 1	25
4.2.5	Instrumental setup for Experiment 2	26
4.3	Sampling	27
4.3.1	Monitoring growth	27

4.3.2	Measurement of photosynthetic parameters using aqua pen	28
4.3.3	Nile Red staining	28
4.3.4	Chla fluorescence measurement	29
4.3.5	Nile Red fluorescence Measurement	29
4.3.6	Dry Weight filtration	30
4.3.7	Chlorophyll absorption spectra measurement	31
4.3.8	Chlorophyll concentration measurement	31
5	Statistical analysis	32
6	Results	32
6.1	Experiment 1	32
6.1.1	Exponential growth data	33
6.1.2	Growth-Irradiance curves	36
6.1.3	Chla vs. dry weight measurement	41
6.1.4	Nile Red vs. dry weight measurement	42
6.2	Experiment 2	45
6.2.1	Growth Monitoring	45
6.2.2	Nile Red fluorescence measurement	46
6.2.3	Lipid Growth Model	49
7	Discussion	53
7.1	Exponential phase growth data	53
7.2	Effect of photo period and irradiance on the growth of <i>P. tricornutum</i>	53
7.3	Growth Irradiance Curve	55
7.4	Effect of Photoperiod and Irradiance on Chlorophyll content	56
7.5	Effect of Photoperiod and Irradiance on Lipid content	57
7.6	Stationary phase growth data	58
7.7	Lipid Variation Per day	59
7.8	Lipid Growth model and validation	60
8	Conclusions	62

References

Appendices

Appendix1. T2- nutrient media composition.

1 Introduction

1.1 World Energy Outlook

The world annual world primary energy consumption increased by 1.8% in the year 2012 (World Energy Outlook, 2013). Fossil fuels accounted for more than 81.4% of total primary energy consumption in year 2011, with oil (31.3%) coal (28.8%) and the natural gas (21.3%) as the major fuels, while nuclear energy and hydroelectricity also accounts for 5.1% and 2.3% respectively (World Energy outlook,2013). Fossil fuel combustion accounts for approximately 99% of total global CO₂ emissions, excluding those from forest fires and the use of wood fuel (EDGAR 4.2, JRC/PBL, 2011). The rise in actual global CO₂ emissions increased by 4.2 % during 2011, and reached 34.5 billion tons in 2012. The main sources of CO₂ emissions are fossil fuel combustion for transport, electricity and thermal energy generation, and other small industrial sources. Moreover, the increase in CO₂ is mainly due to energy-related human activities over the past decades determined by economic growth in emerging countries like China and India (EDGAR 4.2, JRC/PBL, 2012). Due to the emission of large amount of green house gases (GHGs) and associated global warming the search for renewable energy resources has become increasingly popular. For example, the EU has set a target to achieve 20% reduction in fossil fuel use and replace it by 20% use of renewable energy sources by 2020 as well as to replace 10% of the fossil fuel use in road transport mainly with biodiesel (World Energy Outlook, 2013).

To meet the EU 2020 target, a selection of wide range of effective technologies and renewable energy sources are major areas of focus these days. Although renewable energy sources such as nuclear, photo voltaic, wave, hydroelectric and wind energy are becoming increasingly popular as alternative sources, they cannot necessarily fulfill the demand of fuel in the transport sector (Parmer et.al 2011). According to IEA (2011), transportation sector alone accounts for 62.3% of fossil oil consumption compared to other energy sources. As a result, transportation covers a significant share approximately 22% of global fossil fuel combustion-related CO₂ emissions (Oliver et.al, 2013). Thus, biofuel stands out as the ideal solution, and it could be rapidly implemented as it will reduce not only the dependency on fossil oils but also reduce the CO₂ emissions of the transportation sector.

1.2 Biofuel as energy feedstock

To offset the growing energy crisis and associated global warming due to CO₂ emissions, alternative sources of biofuels have already been studied for half a decade's (Konthe et.al 1997). The first generation oil crops for example, rapeseed oil, sugarcane, sugar beet and maize (FAO, 2008) has already attained commercial production of biodiesel in Brazil and USA. The use of first generation biofuels has been controversial from the very beginning because of their impact on the global food market and food security mainly within the vulnerable regions of the world economy (Brennan and Owende, 2009). With its growing use in agricultural lands, the use of first generation crops as biofuel has also raised a question about its potential of replacing the fossil fuels and its sustainability (Moore 2008).

Currently, about 1% of world's available arable land is used for the production of biofuels, providing 1% of global transport fuels (Brennan and Owende, 2009). Despite the controversies, the search for alternatives of biofuel has not slowed down. Second generation biofuel have been introduced with an intention to produce fuels from whole plant matter of dedicated energy crops or agricultural residues, forest harvesting or wood processing waste (Moore et.al,2008), rather than from food crops. However, this technology has not yet reached commercial production.

To make the biofuel technically and economically viable, the alternative should be competitive and cost less than petroleum fuels; they should not require arable land and should enable air quality improvement, low CO₂ emissions, and minimal water use (Khosla et.al, 2009). Exploitation of microalgae could meet this requirement and also meet the primary energy demand, simultaneously providing environmental benefits like CO₂ sequestration (Wang et.al, 2008).

1.3 Microalgae as energy feedstock

Although the idea of using microalgae as a source of fuel is not new (Konthe et. al.1997), large scale commercial production of microalgae is not yet global. Recently, the need of alternative source of energy and growing population has attracted the investors and researchers towards green energy. And micro-algae stands out as a potential candidate for biofuel due to its metabolic flexibility, high oil content to replace

fossil fuels and its cultivation ease at minimal land area. Several other features of microalgae like CO₂ sequestration, waste-water treatment, H₂ production also being studied.

Microalgae are diverse group of photosynthetic micro-organisms that have been reported to double their biomass during exponential growth in one day (Chisti, 2007). Unlike other sources of biofuel, cultivation of micro-algae does not require the fertilized agricultural lands and can convert the fertilizers with 100% efficiency. Several researches have been done for an ultimate search of oil source in plants. Table1 shows the comparison of several oil crops and their oil content and the land area needed for their cultivation based on experimentally demonstrated biomass productivity in photo bioreactors (Chisti 2007).

Table 1. Common sources of biodiesel including microalgae and their oil yield. (Chisti, 2007)

Crop	Oil yield (L/ha)	Land area needed (M/ha) ^a	Percent of existing US cropping area
Corn	172	1540	846
Soybean	446	594	326
Canola	1190	223	122
Jatropha	1892	140	77
Coconut	2689	99	54
Oil palm	5950	45	24
Microalgae ^b	136,9	2	1,1
Microalgae ^a	58,7	4,5	2,5

Note: ^a for meeting 50% of all transport fuel needs of USA

^b 70% oil (by wt) in biomass.

^c 30% oil (by wt) in biomass.

Table 1 shows that microalgae are the source of biodiesel that has the potential to replace the fossil fuels. It appears that oil productivity of microalgae exceeds the oil productivity of oil producing higher plants. Microalgae has been reported to double their biomass within 24 hr. (Chisti,2007) and oil content can exceed by 80% by weight of dry

biomass(Metting,1996;Spolaore et.al.,2006).Oil productivity is the mass of oil produced per unit volume of the microalgal broth per day depends on the algal growth rate and the oil content of the biomass (Chisti, 2007).However, depending upon the species and growth conditions, a variety of lipids can be produced, including the hydrocarbons and TAGs suitable for biodiesel production (Singh et.al, 2011).

Table 2 shows the potential microalgae species that contain high amount of lipids. It has also been reported that a strain of algae if put into a nitrogen-deficient condition, the oil content can increase from 22% to 58% of the oil content per dry mass (Sheehan et al. 1998).The obtained oil can be extracted from the microalgae by using solvent extraction methods and turned into biodiesel through a process known as transesterification (Vasudeva and Briggs, 2008).

Table 2. Lipid content in microalgae species (Singh et.al, 2011; cited from Smith, 2012).

Microalga species	Lipid Content(wt%(w/w))
<i>Botryococcus braunii</i>	25–80
<i>Chlorella emersonii</i> ***	25–63
<i>Chlamydomonas reinhardtii</i>	21
<i>Chlorella protothecoides</i>	14–58
<i>Dunaliella salina</i>	6-25
<i>Dunaliella tertiolecta</i> ***	16–71
<i>Monallanthus salina</i>	> 20
<i>Nannochloris sp</i>	31–68
<i>Phaeodactylum tricornutum</i> ***	18–57
<i>Scenedesmus obliquus</i> ***	11–55
<i>Spirulina platensis</i> ***	4-16

*** (Varfolomeev and Wassweman, 2011)

Algae are also capable of producing biofuel other than biodiesel. Besides, direct burning of algal biomass, waste biomass can be fermented for generation of biomethane and bioethanol (Parmer et.al 2011) (Collet et.al 2011) and some species have also shown to produce hydrogen via activity of chloroplastic hydrogenase powered by reductive reactions derived from photosynthesis. A few species have been shown to produce hydrocarbons (similar to kerosene) (Park et.al, 2005) and few cyanobacteria ca-

pable of secreting ethanol. Thus, algae species have shown a great potential for biofuel and finding different ways of exploiting these tiny organisms might bring a great advantage. Therefore, efficiency may require genetic engineering on multiple parts of metabolism and understanding of growth kinetics to manipulate micro-algae in near future (Bonente et.al, 2011).

Despite of all these advantages, the cultivation and production cost for microalgae still remains as one of the main bottlenecks in large scale production. And since microalgae are photosynthetic organisms, the efficient use of light is a pre-requisite for successful industrial production processes. Production of sustainable biofuels from microalgae has shown to be one potential option to develop renewable energy. One of the major obstacles that obstruct the commercialization of micro-algal biofuels is the high cost of photo bioreactor and the high demand of auxiliary systems or the intensive energy input required during the cultivation of microalgae.

The main aim of this thesis is to point out the importance of microalgae fuel as an alternative source to replace fossil fuels. Although, algae fuel has been said to be an alternative, there are several biological and technical aspects related to microalgae cultivation that has limited its commercial production. To make the algae fuel economical and feasible, an experimental study was carried out at the laboratory to determine and quantify the effects of light irradiance and photoperiod on growth and lipid content in the chosen species of microalgae. The chosen species is proven to have high lipid content (18-57 wt. %). In a long run, the results will be useful to understand the production limits for scale up cultivation globally.

2 Literature Review

2.1 Microalgae

Microalgae are a group of polyphyletic organisms with unicellular origin. They are mainly aquatic and water dwelling organisms lacking complex morphological organization. These unicellular organisms are capable of evolving O_2 through the use of photosynthetic pigments, have a range of cell sizes (2-200 μ m) and are autotrophic and heterotrophic in nature.

Traditionally, micro algae have been classified according to their color (i.e., green algae (Chlorophyta), brown algae or diatoms (Bacillariophyta), red algae (Rhodophyta), and blue green algae or cyanobacteria. However, the classification is nowadays based on genetic relationships, composition of the chloroplast, pigments, storage products, cell wall composition and several other morphological and genetic characteristics. Diatoms are one of the most important micro-algae classes. Diatoms are autotrophs which require light, CO_2 and inorganic nutrients to synthesize into organic carbon. The term algae in this thesis refers to microalgae or a diatom.

2.1.1 Morphology

Diatoms are unicellular (1-200 μ m), although they can exist as colonies too. Diatoms have diplontic life cycle with a prolonged vegetative phase during which the cells divide mitotically. The cell wall of diatoms consists of polymerized silicon and is surrounded by plasma membrane as shown in Figure 1. The major organelles inside a diatom cell include nucleus, mitochondria, vacuole, chloroplasts and other cell organelles depending on the species. The major photosynthetic organ is chloroplasts which contain light sensitive chlorophyll pigments such as chlorophylls a and c, beta carotene, fucoxanthin and diatoxanthin. The major storage compounds of diatoms are lipids (TAGs) and a β -1, 3-linked carbohydrate known as chrysolamarin.

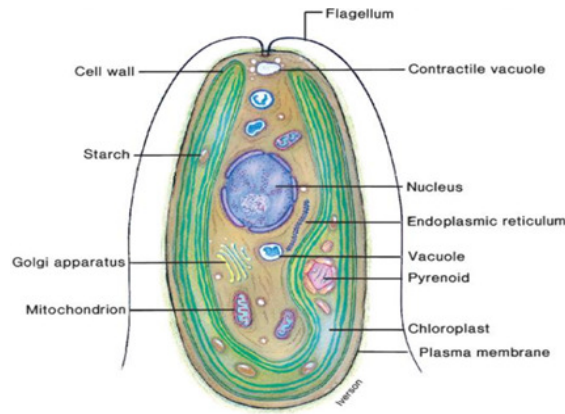


Figure 1. Morphology of a microalgae cell (McGraw-Hill companies, Inc.)

2.1.1.1 Algae growth dynamics

The growth dynamics of an axenic culture of microalgae can be divided into five different phases as shown in Figure 2.

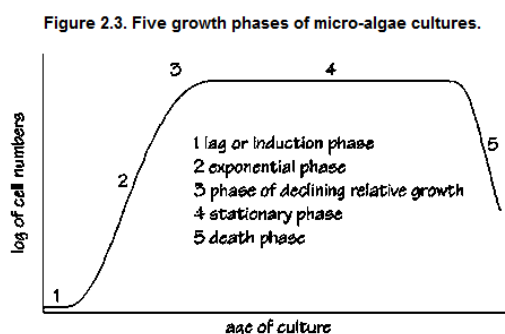


Figure 2. Five growth phases of the micro algae culture (FAO).

The lag phase occurs just after inoculation of new culture before the cells are acclimated to new growth conditions. If the cells are transferred from different culture medium or reactor vessel or light condition, it takes some time before the cell division starts. As, the cells start to divide, cell density or number of cells starts to increase exponentially which is called log or exponential phase.

In the third stage, the culture conditions change and the limiting factors interfere with the cell growth. Factors such as light availability due to mutual shading and oxygen accumulation caused by photosynthesis limit the cell growth. After the cell division slows down, the stationary phase occurs and the lipid accumulation takes place. The

accumulation of lipids in microalgae cells is due to a shift in their metabolism and can be triggered by adverse conditions such as nutrient depletion. This phenomenon is observed in many of the algae species. In the fifth stage, the culture media starts to deteriorate, and the nutrient level starts to deplete to a level which is incapable to sustain growth. In this stage, the culture eventually collapses. The key to the successful algae culture is to maintain the cultures in the exponential phase of growth.

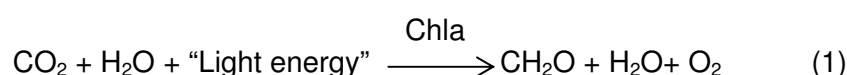
2.2 Factors affecting growth of microalgae

2.2.1 Light supply

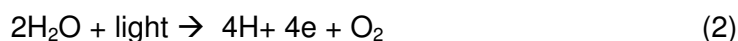
Light is an essential factor for microalgal growth. Light in the form of solar energy drives photosynthesis in phototrophic organisms. However, not all the lights available are used by the cells for photosynthesis. Photosynthetic pigments in microalgae can utilize mainly the visible light between 350 and 700nm, which is roughly 50% of global irradiance (Seppälä et.al, 2012).

2.2.1.1 Photosynthesis in microalgae

Microalgae are oxygenic photoautotrophic microorganisms. They use sunlight to metabolize carbon dioxide (CO₂) inside energy rich organic compounds (CH₂O) under liberation of oxygen (O₂). CH₂O is organic compound that are used as building blocks for microbial growth. The generalized form of photosynthesis is written as follows:



Where, Chla is the ubiquitous plant pigment chlorophyll a. Equation 1 implies chlorophyll-a catalyzes a reaction or series of reactions whereby light energy is used to oxidize water: yielding gaseous molecular oxygen. The end products of photosynthesis are carbohydrate molecules, proteins, enzymes and lipids.



As mentioned earlier, not all the incoming solar radiation is used by algae for photosynthesis. The primary pigment Chla involved in photosynthesis has absorption bands in

the region of 400-500 nm and 650-700 nm. This limits the useful radiation to 400-700 nm which is considered to be photosynthetically active radiation (PAR). PAR equals to roughly 40-50% of incoming solar irradiation (Peter.et. al 2010). A study by Spilling and Seppälä (2012) suggests the total energy losses during the process of photosynthesis in Figure 3.

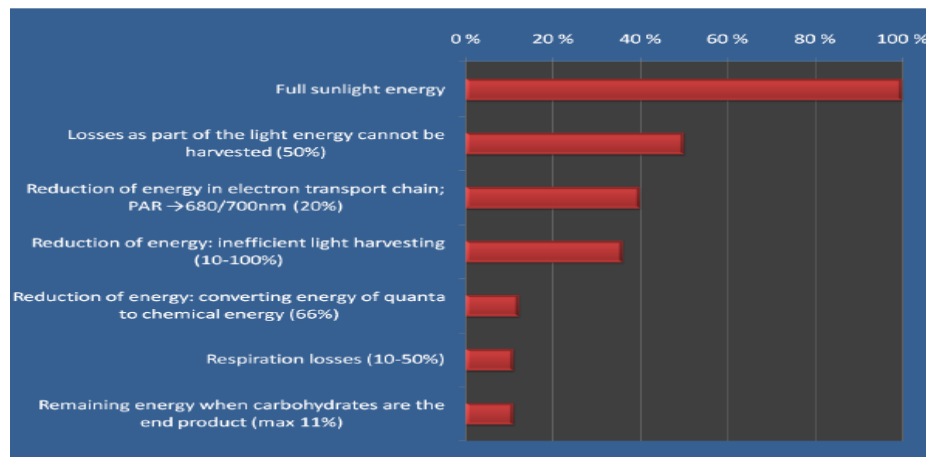


Figure 3. Factors affecting energy conversion during photosynthesis from solar irradiance to organic matter in microalgae. (Seppälä, 2013)

A large fraction of the total incoming energy is lost during the process of photosynthesis. Only 50% of the incoming solar energy can be harvested by the photosynthetic pigment in microalgae and other higher plants. Apart from that, approximately 20% reduction in energy occurs in the electron transport chain. The reduction is mainly due to the cumulative energy contained by all absorbed light quanta being used to match the energy of the same amount of red light quanta. Moreover, the reduction also depends on the efficiency of light harvesting and utilization of photo systems, which can be roughly 10-100%. This efficiency, can, however, depend upon the species and culture conditions. The other factors affecting the energy conversion include respiration losses of (approx. 10-50%) and energy reduction during the conversion of light energy to chemical energy (approx. 66%). Even if the losses were kept to the minimal level, only 11.5% of total energy could be obtained from the bi-product carbohydrate as energy. (Spilling and Seppälä, 2012)

Taking all the losses into account, the photosynthetic efficiency can be even smaller; efficiencies in the range of 1-5 % have been recorded as the best cases so far. Nevertheless, photosynthetic efficiency of targeted species and genetic exploitation and con-

trol of culture condition can certainly be productive when opting for large scale real production systems.

2.2.1.2 Solar irradiance and photosynthetic efficiency

Solar irradiance is considered as the most influencing factor for the growth of phototrophic microalgae as it drives photosynthesis. According to Darzins.et.al (2010), a solar radiation of approximately $1500 \text{ kWh.m}^2 .\text{y}^{-1}$ is considered adequate for algae cultivation. The global solar irradiance averages map indicates the majority of the earth's land surface is suitable for algae cultivation as shown in Figure 4, but in practice, significantly less of this land is actually suitable for year-round cultivation. An ideal algae production system requires year-round low variations in solar irradiance, temperature and seasonal changes.

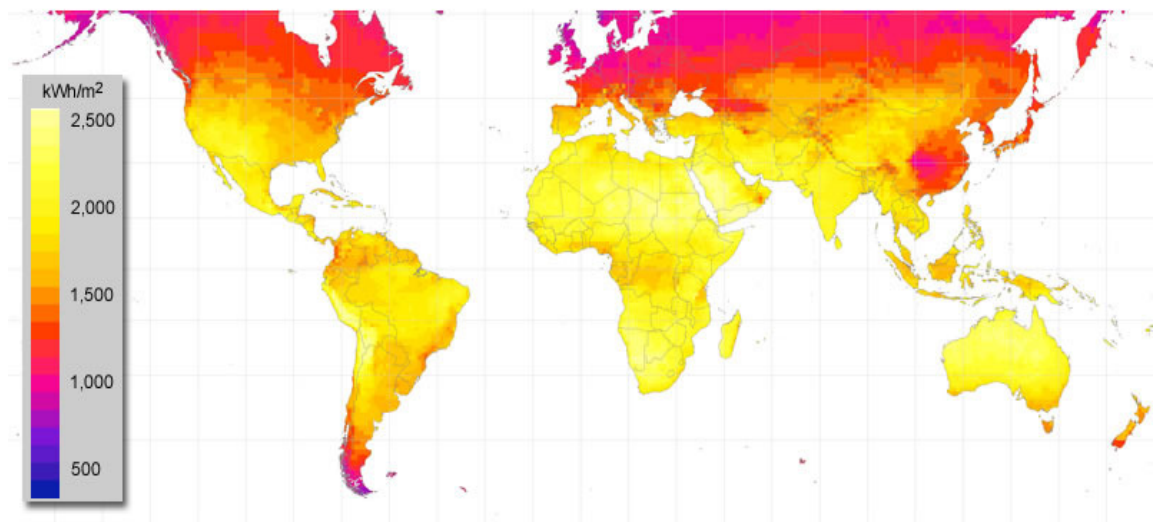


Figure 4. Yearly sum of global irradiance averages over the period of 1981 to 2000. (Meteonorm)

As much as solar irradiation influences growth, it also limits the growth called photo saturation, when a level is reached. Photo saturation essentially is because the light harvesting antenna pigment has been optimized for the daily average intensity of incoming irradiation. At high irradiation conditions, photons are harvested at a rate much faster than the rate at which the reaction centers can process them. In this condition, there is no further increase in photosynthesis; rather, damage in photosynthetic apparatus may occur due to excess energy absorption leading to photo inhibition. Photo inhibition is dependent on both the intensity of light and the photoperiod. In many

freshwater and marine microalgae, irradiances of $100\text{--}200\ \mu\text{mol}\cdot\text{q}\cdot\text{m}^{-2}\cdot\text{s}^{-1}$ range may lead to photo saturation or even photo inhibition. Light saturation and photo inhibition are often the bottlenecks in maintaining high photosynthetic efficiency in micro algal cultures under natural illumination. (Tredici, 2010)

Figure 5 shows the potential yield of algae biomass at 5% photosynthetic efficiency globally. Geographical areas with high irradiance all year long are considered to be the optimal condition for microalgae cultivation. Microalgae biomass productivity is the highest in the warm countries close to the equator where seasonal light levels and temperatures do not vary much, while the higher latitude areas are the ones with lowest productivity. The main reason for this variability is the large seasonal changes in higher latitude regions for algal growth. In such areas, it would be critical to identify the local strains that grow best at lower light exposure and irradiances, while maintaining the optimum growth rates and yields. Israel, Hawaii and Southern California have been home to commercial microalgae farms till date. (Tredici, 2010)

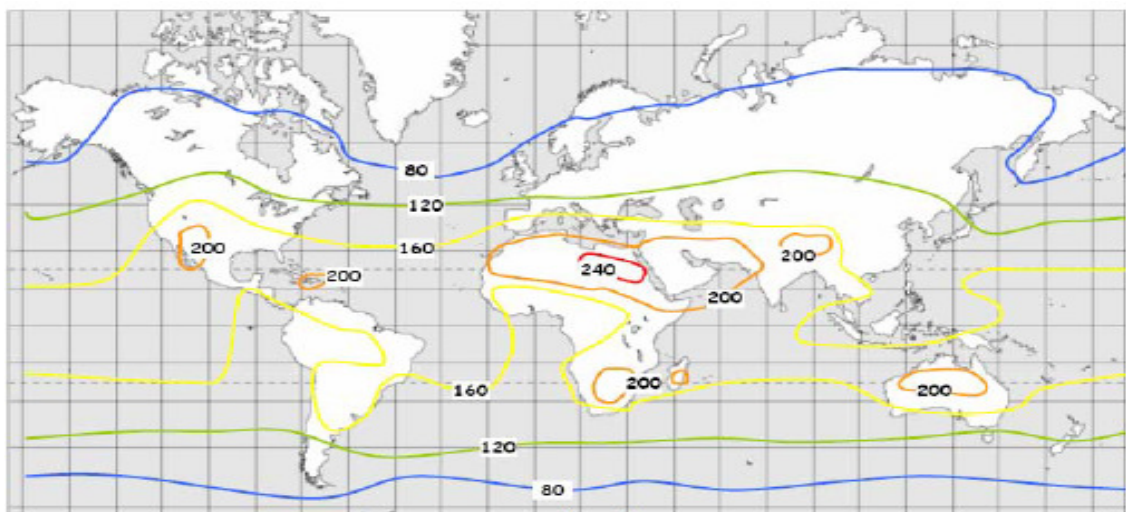


Figure 5. World map of algae biomass productivity ($\text{tonnes ha}^{-1} \text{ year}^{-1}$) at 5% photosynthetic efficiency considering energy content at $20\ \text{MJ Kg}^{-1}$ dry biomass (Tredici, 2010).

2.2.2 Nutrients

Nutrients are another important factor for micro algal growth. Microalgae use nutrients along with light energy to synthesize inorganic compounds into organic compounds. The nutrient media includes nitrogen, phosphorus and carbon (Richmond 1988) and

each micro algal species tend to have their own optimum nutrient content (Maddux and Jones 1964, Rhee and Gotham 1981, Smith 1983, Conar and Fallow field 1997).

Lipid accumulation in microalgae is mainly favored under stress conditions such as nutrient starvation, light limitation and pH variations. Among those stress conditions, nitrogen limitation is one of the most effective and commonly used strategies for stimulating lipid accumulation in microalgae. It is said that when micro-algae are cultivated under nitrogen starved conditions, the proteins in microalgae will be decomposed and converted into energy rich products such as lipids. Studies by Siaut et.al (2011) found that starch would be first synthesized to reserve energy, then lipid would be produced as long term storage mechanism in case of prolonged environmental stress (such as nitrogen deficiency) .

Phosphorus also plays an essential role on cell metabolism and regulation (Droop 1973, Smith 1983). It is used to synthesize enzymes, phospholipids and energy supplying compounds such as AMP, ADP and ATP (Talyor 1987, Beardall et.al. 2001).CO₂ is another important nutrient that is critical for photosynthesis in microalgae. Microalgae in reaction with light energy convert CO₂ into organic compounds and water. Other nutrients such as Mg²⁺, K⁺ and Ca²⁺ also play a vital role in the growth and metabolism of microalgae. Moreover, trace elements and vitamins are also required by microalgae for growth. For example, copper (Cu⁺), iron (Fe⁺⁺) and zinc (Zn⁺⁺) as trace metals are essential for facilitating some enzymatic function such as carbonic anhydrase catalysis (Brand, et al.1983, Lage et. al 1994, Morel et.al 1994, Buitenhuis et.al 2003).

2.2.3 Temperature

After light, temperature is the next limiting factor for micro algal growth in both closed and open outdoor systems to maintain productivity (Richmond 1987, 1988, Richmond et.al 1990, Torzillo, et al 1991). Microalgae can tolerate a range of temperatures and their response to temperature variations can affect their nutritional requirements, rates and nature of metabolism, cell composition (Richmond 1999).

Most microalgae can easily tolerate temperatures up to 15 °C lower than their optimal temperature but exceeding the optimum temperature by only 2 to 4 °C may result a total loss of the algal culture (Richmond 1999).Thus, a successful commercial produc-

tion of microalgae requires a temperature range and suitable climatic conditions for the chosen species.

2.2.4 pH

pH is another important environmental parameters for microalgal growth and productivity. The pH values of cultures can affect the biochemical process associated with microalgae including the bio-availability of CO₂ for photosynthesis and the use of nutrient media (Pandey et.al, 2013). The optimal pH for most cultured microalgae species is between 7 and 9 (Ho et.al., 2011). Hence, it is crucial to maintain the culture pH in the optimal range because culture collapse may occur due to the disruption of cellular processes in extreme pH. pH is often regulated by CO₂, increasing CO₂ decreases pH in the culture. In addition, the photosynthesis also consumes CO₂, which increases pH, thus, should be controlled.

2.2.5 Salinity

Salinity can affect the growth and cell composition of microalgae (Gomez, et.al 2003). Changes in salinity affect the algal growth normally in three ways: 1) osmotic stress 2) ion (salt stress) and 3) changes of the cellular ionic ratios due to the selective ion permeability of the membrane (glass 1983, Brand 1984). The salinity condition may affect the production of specific components in microalgae.

2.3 Algae cultivation principles

Microalgae can be cultivated in the laboratory or in an industrial or aqua cultural station using aqueous media containing nutrients required for growth and exposed to suitable light, temperature and aeration conditions. There are two main principles for algae cultivation: batch and continuous culture (Lee and Shen 2004, Fogg and Thake, 1987).

In a batch culture, at a certain point micro algae starts to grow, the cell density starts to increase and the culture reaches to the stationary phase. After reaching the stationary phase, the algae can be harvested for lipid production. In a batch culture, the five natural growth phases and the metabolism of microalgae can to a certain extent be simu-

lated (Fog and Thake, 1987) which could be very useful in commercial production of microalgae. Microalgae cultivation in batch culture is relatively simple to set up, and large numbers of cultures can be grown simultaneously.

In contrast, in a continuous system, the algae grows and the fresh medium is added while an equal volume of culture (medium plus organism) is removed and the system continues until a steady state phase is achieved (Fogg and Thake et al 1987). To maintain the high productivity and to optimize the culture conditions, the culture needs to be monitored during cultivation (Sandnes et.al 2007, Lee and Shen 2004). The irradiance, temperature, pH and gas composition of the culture have to be controlled and the biomass has to be estimated (Fogg and Thake et al, 1987).

Choosing the best biomass production method or a system also depends on the selected algal strain and its integration with appropriate downstream processing, which is the means for attaining affordable and scalable biodiesel production.

2.4 Commercial scale cultivation

2.4.1 Open and raceways ponds

Microalgae cultivation can be done in open and shallow ponds with a proper mixing and aeration system. Open ponds were the first cultivation technology for mass cultivation of microalgae since the 1950s (Chisti 2007).

The system consists of a circuit of parallel tunnels placed at ground level in which the microalgae suspension flows gently. The mixing and circulation is done by the paddle-wheel as shown in Figure 6. The system can be built in concrete or ditch dug into the ground and can be lined with white plastic sheets. In this system, the water levels are kept at no less than 15 cm and algae are cultured under conditions identical to their natural environment. The pond is designed as a raceway configuration as shown in figure 6. (Chisti, 2007)

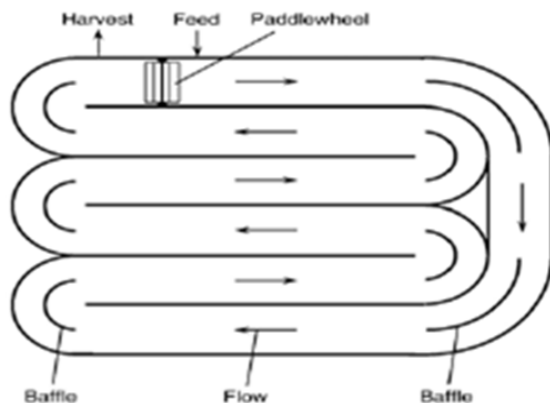


Figure 6. Schematic diagram of open raceway algae cultivation system (Chisti 2007).

Open system cultivation has several advantages as they are cheaper, relatively easier to clean and maintain and need only small energy inputs (Brennan and Owende 2010). In open raceways, cooling is only achieved by evaporation. Thus, the system is highly sensitive to diurnal cycle and seasonal changes (Chisti, 2007). Moreover, raceway ponds are subjected to contaminations and temperature fluctuations (Brennan and Owende 2010, Chisti 2007, Molina Grima 1999). Also, salinity changes due to evaporation and dilution due to rainfall could be quite a nuisance in such cultivation systems (Schenk et al 2008, Chisti 2007). Major commercial farms in California, Hawaii, Australia and Israel have been relying in this method for over 30 years (Chisti 2007).

2.4.2 Closed photo bioreactors

Photobioreactors (PBRs) are flexible, closed cultivation systems that can be optimized according to the biological and physiological characteristics of algal species (Mata et al 2009). In a PBR cultivation system, the direct exchange of gases and contaminants between the cultivated cells and atmosphere, and the amount of impinging light entering the cultivation system are limited by the walls of the bioreactor (Teresa et al 2009). Generally, PBR consists of an array of straight glass or plastic tubes as shown in Figure 7. The tubular array captures sunlight and can be aligned in many different ways e.g. horizontally, vertically, inclined and also as helix (Molina Grima et al 2001, Sanchez et al 1999, Ugwu et al 2002, Wantanbe et al. 1997). PBR containers are made up of transparent materials such as plastic or glass (Chisti 2007). A simple schematic diagram of PBR is presented in Figure 7.

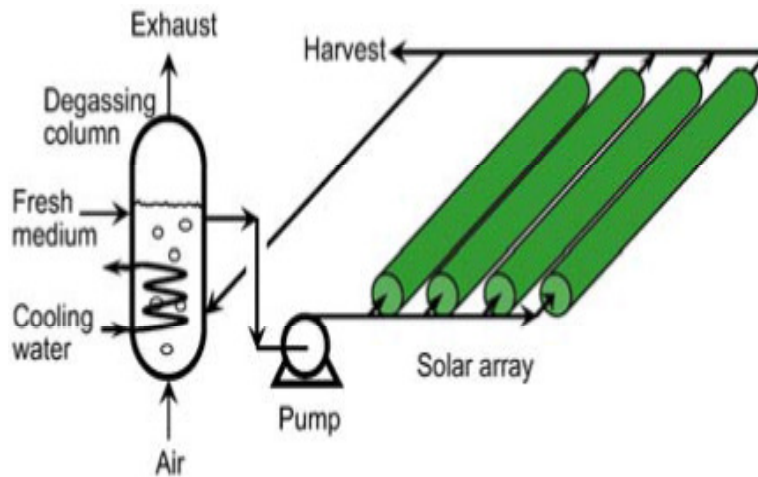


Figure 7. A schematic diagram of a photobioreactor (Chisti, 2007).

In a photobioreactor, the cultivation vessels have a large surface area-to-volume ratio. The most widely used PBR is a tubular design which has a number of clear transparent tubes, usually aligned with the sun rays (Chisti 2007; Tredici et.al, 2010). The tubes are generally less than 0.1 m in diameter to maximize the sunlight penetration to the cultures (Teresa et al, 2009). The culture is circulated through a pump to the tubes where it is exposed to light for photosynthesis and then returned back to the reservoir. A portion of algae is harvested, after it passes through solar collection tubes, making continuous algal culture possible (Chisti 2007).

In closed PBRs, the culture must be periodically returned to the degassing zone an area where the algal broth is bubbled with air to remove excess oxygen (Chisti and Moo-Young, 1993; Chisti 1998). In addition, CO₂ must be fed into the system in order to successfully cultivate the microalgae on a larger scale. As the entire cultivation system is exposed to the sunlight, overheating occurs within the tubes and hence, requires cooling and temperature regulation during daylight hours (Chisti, 2007). PBR also poses several disadvantages such as overheating, bio-fouling, oxygen accumulation, difficulty in scaling up and cell damage by shear stress etc. (Ugwu et.al, 2008). Nevertheless, several designs are being researched to optimize PBRs according to the species and their culture conditions and cultivation.

2.5 Algae Lipids

Lipids, in simple terms, are defined as biological molecules that are soluble in most organic solvent. Most lipids contain fatty acids and are classified into two categories based on the polarity of the molecular group: polar lipids and neutral lipids (Kate's 1986a). Polar lipids are packed in parallel to form a bilayer cell membrane (Halim et.al, 2012). Polar lipids are further subcategorized into phospholipids (PL) and glycolipids (GL) (Halim et. al, 2012).

Neutral lipids are primarily used as energy storage in the micro algal cells (Halim et al, 2012). Neutral lipids comprise of acyl glycerol and free fatty acids (FFA). A fatty acid (FA) molecule consists of a hydrophilic carboxylate group attached to one end of a hydrophobic hydrocarbon chain. Both polar and neutral lipids consist of fatty acid molecules that are categorized based on the two important features: the total number of carbon atoms and the number of double bonds in the hydrocarbon chain (Halim et.al 2012). The neutral lipids are formed when the carboxylate end of the fatty acid molecule bonded to the uncharged head group of glycerol (Halim et.al, 2012). In contrast, polar lipid molecule is formed when a fatty acid molecule is attached to a charged head group of glycerol and phosphate complex (Halim et.al, 2012).

Acyl glycerol consists of fatty acids ester bonded to glycerol backbone and is classified according to its number of fatty acids: triglycerols (TG), di glycerols (DG), mono acyl glycerols (MG). Acyl glycerol is desirable for commercial scale biodiesel production mainly for two reasons. Firstly, industrial-scale alkaline-catalyzed transesterification is designed to process acyl glycerols (TG, DG and MG) and has limited efficacies on both lipid fractions i.e. polar lipids and free fatty acids (Chisti, 2007, Lang.et.al, 2001). Secondly, because acyl glycerol has a lower degree of unsaturation than other lipid fraction such as polar lipids and they produce FAME with higher oxidation stability (Halim et.al, 2012).

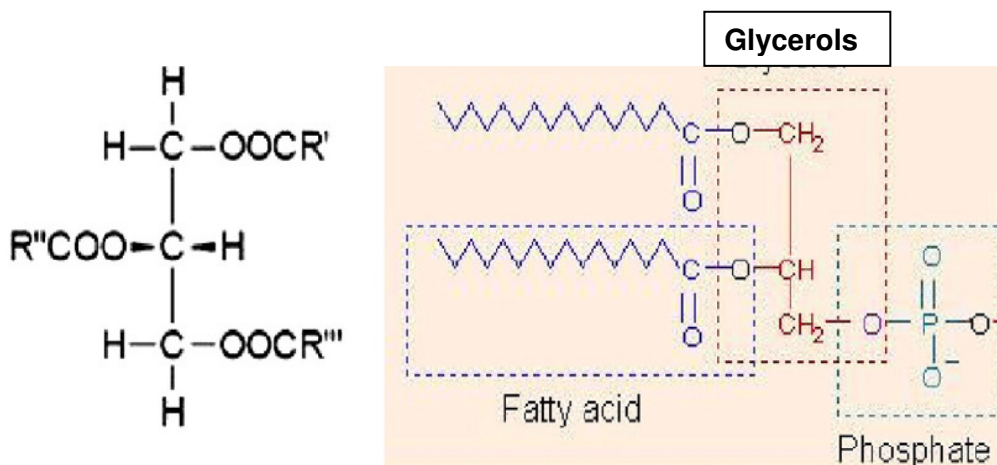


Figure 8. Tri glycerol (neutral lipid) and phospho lipid (right). Symbols R' R'' and R''' represents the tri-glycerol molecule with three fatty acid chains (Nelson and Cox, 2000).

Microalgal fatty acid contains 12 to 22 carbons in length and can be found in saturated or unsaturated form. Saturated fatty acids have no double bonds while unsaturated fatty acids have at least one double bond (Nelson and Cox, 2000). The number of double bonds in the fatty acid chains does not exceed 6 and most of all of the saturated fatty acids are cis-isomers (Medina et.al, 1998).

Micro algal lipid content varies from one species to another in terms of biomass from 5 to 77wt% (Chisti 2007, Brown et.al 1997). The composition and fatty acid profile of lipids extracted from particular species is also affected by micro algal life cycle and the cultivation conditions like: medium composition, temperature, illumination intensity, photoperiods and aeration rate (Rao et.al, 2007; Guzman et.al 2010; Ota et.al, 2009, Ramadan et.al, 2008). However, the accumulation of lipids in micro algal cells can be triggered by adverse conditions such as nitrogen-depletion (Hu et.al 2008, Rodolfi et.al 2009, Pruvost et.al 2009). Under such conditions, the largest fraction of these lipids consists of TAG is found. These TAGs may accumulate up to 43% of micro algal dry weight and are very rich in saturated fatty acids. TAGs are more useful for conversion into biodiesel (Meng .X et.al, 2009).

It is said that even with a higher lipid content the net oil produced may actually decrease in a nutrient stressed condition due to significantly reduced cell concentration. (Sheehan et.al 1998, 20-22). Nevertheless, a better understanding of this growth kinet-

ics could be possible to increase the net increase in total oil productivity by carefully controlling the timing of nutrient depletion and cell harvesting.

3 Algae biomass harvesting techniques

Separating the algae from water has proven to be one of the bottle necks (both physical and economic) to industrial scale processing partly because of the small size of algal cells of unicellular eukaryotic algae which is typically 3-30 micrometers (Grima et.al 2003). The techniques of recovering microalgae biomass from the culture medium can contribute to 20-30% of the total cost of biomass (Teresa et.al, 2010).

Micro algal properties that simplify the harvesting are large cell size, high specific gravity compared to that of medium, and autoflocculation. Also, the best harvesting method should have minimal energy consumption and be as economical as possible. Common harvesting techniques for micro-algae biomass are sedimentation, centrifugation, and filtration, ultra- filtration, sometimes with an additional flocculation step or with the combination of flocculation- flotation. However, the harvesting method usually depends upon the strains of the microalgal species and the final product desired. (Chisti et. al; Pandey et.al. 2013)

Effective dewatering techniques are required to achieve maximum lipid extraction. High density algal cultures such as those in reactors can be concentrated by either chemical flocculation or centrifugation. The oil is usually extracted using solvent i.e. hexane (Grima et.al, 2003).

3.1 Filtration

Filtration is a physical separation process in which the particles in the suspension are retained using a filter. The filter is highly efficient and safe in the solid and liquid separation process (Pires et.al, 2012). However, this method is only suitable for larger microalgae species but remains unsatisfactory for smaller cells (Ho.et.al 2011). Filter presses operating under pressure and vacuum can be used to recover large quantities of biomass, but for some applications filtration can be slow and inefficient. In addition, membrane microfiltration and ultra-filtration can be two other possible alternatives to

replace conventional filtration for recovering algal biomass, which could be more suitable for fragile cells and small scale production process. (Pandey et.al, 2013)

3.2 Centrifugation

Centrifugation is also seen as the most effective biomass harvesting technique, however, the energy and capital costs associated with the technique is slightly unappealing (Uduman et.al.2010). Centrifugation involves the application of centripetal acceleration to separate the microalgae from the culture medium (Harun.et.al 2010) and is the fastest method to cell recovery method based on the density gradient. The centrifugation disks are easier to clean and maintain, and centrifugation technique can be applied to any species of micro algae (Christenson and Sims, 2011).

3.3 Flocculation

Flocculation is a method to separate the algae from the medium using chemicals to force the algae clump together and come out of suspension in the water, either by floating on the top or by sinking to the bottom of the liquid for easier collection (Yahi et al, 1994, Oh et al. 2001; Gutzeit et.al, 2005; Danquah et.al, 2009, Campbell et.al. 2009). Flocculating agents are the chemicals promoting conglomeration from the solution by causing colloids and other suspended particles to aggregate (Borowitzka et.al 2013).The micro algal cells carry negative charge on the surface to prevent cell aggregation. The negative charge can be altered by adding flocculants (Harun et.al 2010). Flocculation can be done using three methods; Chemical flocculation, Bio flocculation and electro flocculation. Common flocculant types are aluminum sulphate, aluminum chloride and ferric chloride (Chisti, Pandey et.al 2013).Flocculants are toxic if used in high concentrations might not be very feasible to use in industrial production of biomass harvesting. In order to make the process feasible, the flocculants should be cheaper, nontoxic and effective at lower concentrations (Chisti, Pandey et.al 2013).

3.4 Electrophoresis

Electrophoresis is another potential method for separating microalgae without the need for chemicals (Pandey et.al 2013). An electric field directs the microalgae to the exter-

nal part of the solution where algae normally carry negative charge. Electrolysis produces hydrogen which adheres to the microalgae flakes and carries them to the surface. Several benefits of this process are reported as it does not require any chemical and is energy efficient and environmentally compatible (Chisti et. al; Pandey et.al, 2013). However, the high cost of this process has limited the process to the large scale production (Uduman et.al 2010).

Richmond (2004) reported that the main criteria for selecting an appropriate process to harvest algal biomass depend on the type of byproduct desired. In products with low commercial value, sedimentation through gravity with the aid of flocculants can be used. However, high value products such as human food, drugs and aquaculture require continuous operations to produce large volumes of biomass. (Chisti and Pandey et.al, 2013).

4 Experimental

4.1 Aims of the study

This Bachelor's thesis was carried out at the Finnish Environment Institute as a part of SUBMARINER research project 'Potential uses of micro and macro algae in the Baltic Sea Region co-funded by the EU. The project mainly dealt with sustainable use of marine resources in the Baltic Sea Region. Moreover, it partly focused on the cultivation of macro algae for nutrient uptake to remove eutrophication from the Baltic Sea and also on the search for uses of micro algae for sustainable production of algal fuel. The marine laboratory did a major research on the potential applications of algae in the submarine EU project from 2010 till 2013.

The research team studied the effect of temperature, nutrient limitation, salinity, and other environmental factors so as to ease the cultivation and harvesting of microalgae for sustainable production of biofuel. However, it was not understood if the combination of irradiance and photoperiod (light- dark regime) had any effect on the growth rate and lipid production in microalgae. Thus, this thesis was carried out to find out the effects, quantify and design suitable condition for microalgae cultivation.

The first aim was to determine, the effects of light irradiance and photo periods on the growth rate of *Phaeodactylum tricornutum* and to quantify the effect for commercial scale algae cultivation. The experiment was arranged in different photoperiod regimes and was run for 2 weeks. After completion of first experiment, two light irradiance levels and photoperiods were chosen for the second experiment. This experiment resulted in a 2² factorial design. The cells were cultivated in a nutrient limited medium at the stationary phase. Therefore, the main aim of the second experiment was to find out the effects of irradiance and photo period on the variation of lipid content in the chosen species.

The overall aim of the study was to monitor and quantify the effects of irradiance and photoperiods on the algal growth and the lipid content. The results will help in modeling and evaluating the growth with varying light intensities and photoperiods in various locations. In addition, the results will provide a basic understanding of the production limits globally.

4.2 Material and Methods

This thesis project is divided into two distinct sets of experiments. The first sets of experiments were done with varying irradiance $\mu\text{mol}\cdot\text{q}\cdot\text{m}^{-2}\cdot\text{s}^{-1}$ and photo period h. Irradiance and photoperiod were arranged in 4 fixed levels: 400, 180, 40, and 20 $\mu\text{mol}\cdot\text{q}\cdot\text{m}^{-2}\cdot\text{s}^{-1}$ for irradiances and 6 different levels: 4, 8, 12, 16, 20, and 24 h of photoperiods, respectively. The results and outcome will help to examine and understand the behavioral and growth pattern of *Phaeodactylum tricornutum* with respect to changing irradiance and photoperiod. The second experiment was based upon the first experiment where two photoperiod and irradiances level were chosen to monitor and comprehend the varying lipid accumulation in both photo periods.

4.2.1 Species selection

The species were chosen based on a screening study by (Schwenk et al 2013). The diatom *Phaeodactylum tricornutum* TV335 is the brackish water species isolated from rock pools near Tvärminne Zoological Station in Hanko, Finland. The species was chosen because of its growth rate and higher lipid content according to previous studies (Schwenk et al 2013).

4.2.1.1 *Phaeodactylum tricornutum*

Phaeodactylum tricornutum is assigned to the division Chrysophyta and class Bacillariophyceae (Diatoms). Diatoms are microscopic unicellular or colonial (in shape of filaments or ribbons or tube dwelling) eukaryotic algae abundant in most aquatic habitats. Diatoms contribute up to about 20-25% of the world net primary production which puts it in the same position as the Pinaceae in the temperate and boreal forests and the Poaceae (grasses) in the savannas, grasslands and cultivated areas. Thus, they are also characterized as significant primary producers of marine habitats, fresh water and brackish water in polar and equatorial regions.

Phaeodactylum tricornutum exhibit a number of features such as siliceous cell walls, composed of two halves that together with girdle bands form frustule cells. The frustules of diatoms which belong to Bacillariales or (Pennales) are elongated and have

bilateral symmetry. Diatoms are often visible to the naked eye as a golden coating growing on vessels and they commonly form brown films on aquarium glass or rocks.

Diatoms play a key role in carbon fixation in oceans and synthesize carbohydrates that serve as a chief source of zooplankton food in the marine food chain. Due to their ecological significance; diatoms were first cultivated for water quality monitoring and pollution evaluation. And within the diatom species, *P. tricornutum* has been cultivated most frequently.



Figure 9. Microscope pictures of *Phaeodactylum tricornutum* individual cell figure by Alessandra de Martino and Chris Bowler Stazione Zoologica and Ecole Normale Supérieure.

P. tricornutum is classified as a pennate diatom with two forms of cells; oval and fusiform however, only the oval form possesses a silicified raphe (Lewin 1958 et.al); thus, it has been put under class Bacillariophyceae. It is the only representative of suborder Phaeodactylacea, genus *Phaeodactylum* (Lewin 1958, Lewin et al.1958). The cells can be about 10 μm and are non-motile.

The particular species used in this study is *P. Tricornutum* TV335 is fusiform as shown in Figure 9. This species is a brackish water species and has been isolated from rock pools near Tvärminne Zoological station in Hanko, Finland.

4.2.2 Cultivation

The diatom species were cultivated in a 550 ml, 175cm² CellStar tissue culture flasks using T2 Tvärminne media. The composition and concentrations of nutrients, trace metals, vitamins of the used medium are listed in the recipe (see Appendix T2 media recipe), with the only difference that the macronutrients were adjusted to the molar ratio of Si, being only 50% of total composition.

The stock solutions of the culture media containing nutrients, vitamins and trace metals were filtered through 0.2 µm filters (Aero disc 25mm syringe filter) to autoclaved 6 PSU Tropic Marine Salt with Milli RO- water. The batch cultures were continuously aerated and mixed with sterile air (Sera air Pump, 0.2 µm Millipore filters) at 18 ± 1°C in a temperature-controlled cultivation room. In presence of non-limiting nutrients the culture remained mainly controlled by the light irradiance and the photoperiod.

The experiment required an instrumental setup including the LED light panels, light measurement and power setup, continuous air supply using air pumps, dilution and regular sampling as described below:

4.2.3 LED, Light Measurements and Power Setup

SL3500RGB-G-LED units were obtained from Photons Systems Instruments. These LED units have three spectral outputs that peak at wavelengths of 627nm, 530nm and 470 nm for RGB respectively. The light intensity measurement was done in the bottles filled with water using intensity sensor (Spherical Micro Quantum Sensor Us-SQS, Walz) and Light meter (LI250A, Li Cor). Neutral density Screens (Rosco) were used as external wrap around the bottles to limit the total amount of irradiance each bottles received during the experiment. The bottles were arranged in 4 levels of irradiances: 400, 180, 40, and 20 µmol·q·m⁻²·s⁻¹ at 6 levels of photoperiod 4,8,12,16,20,24 h respectively. Day light timer was used to regulate the light hours to the bottles.

4.2.4 Instrumental setup for Experiment 1

Four identical bottles were arranged for the first set of experiment as shown in Figure 10. Each of the bottles contained a silicon stopper with three open needle pipes. The

needle pipes contained a 10 ml syringe, an air filter containing sterile cotton and a pipe leading to the air pump. The syringe was used for sampling, the air filter for air circulation via Sera Air pump, and also, a syringe to bring filter air from the culture media. A similar set-up was used throughout Experiment 1. An experimental setup used in this thesis project is shown in Figure 10.

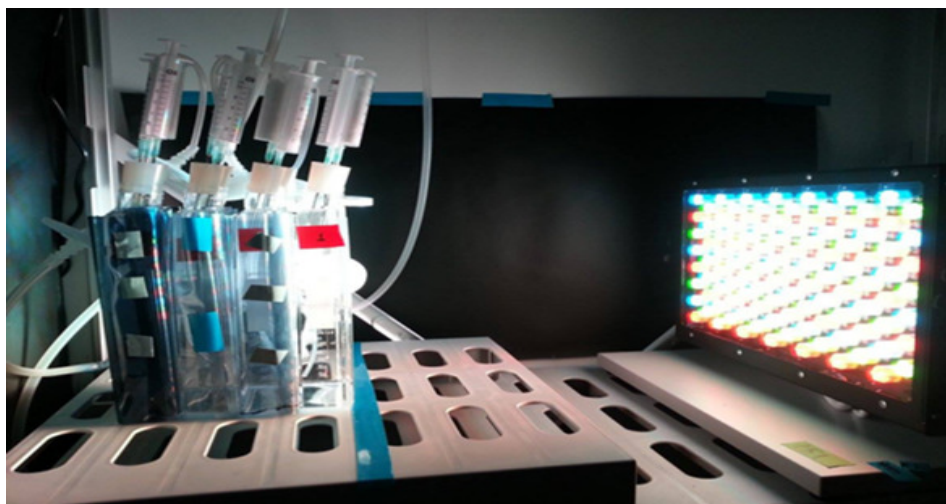


Figure 10. Instrumental set up for Experiment 1

4.2.5 Instrumental setup for Experiment 2

After the completion of first experiment, photoperiod 8 and 20 at irradiance level of $180 \mu\text{mol}\cdot\text{q}\cdot\text{m}^{-2}\cdot\text{s}^{-1}$, $72 \mu\text{mol}\cdot\text{q}\cdot\text{m}^{-2}\cdot\text{s}^{-1}$ were chosen for the study. Two reasonable lower and higher growth rates were chosen to see how the chosen new irradiances and the photoperiods will affect the yield i.e. the lipid content. The experiment resulted in a 2^2 factorial design. The main goal in this study was to monitor and quantify the effect of best lipid accumulation condition on photoperiod vs. irradiance condition. Hence, the chosen species were grown in stationary phase.

The experimental set up was similar as Experiment 1. The chosen species *P. tricornutum* (TV335) were cultivated in two bottles (Nalgene, 2000ml) in N_2 nutrient limited medium (See Appendix) for a week at two irradiance levels $180 \mu\text{mol}\cdot\text{q}\cdot\text{m}^{-2}\cdot\text{s}^{-1}$ and $70 \mu\text{mol}\cdot\text{q}\cdot\text{m}^{-2}\cdot\text{s}^{-1}$, respectively. The temperature and salinity condition of the culture was the same as in the experiment I. The samples were cultivated till the station-

ary phase. The growth rate was monitored daily using FlowCAM. The final arrangement of experiment 2 is as shown in Figure 11.

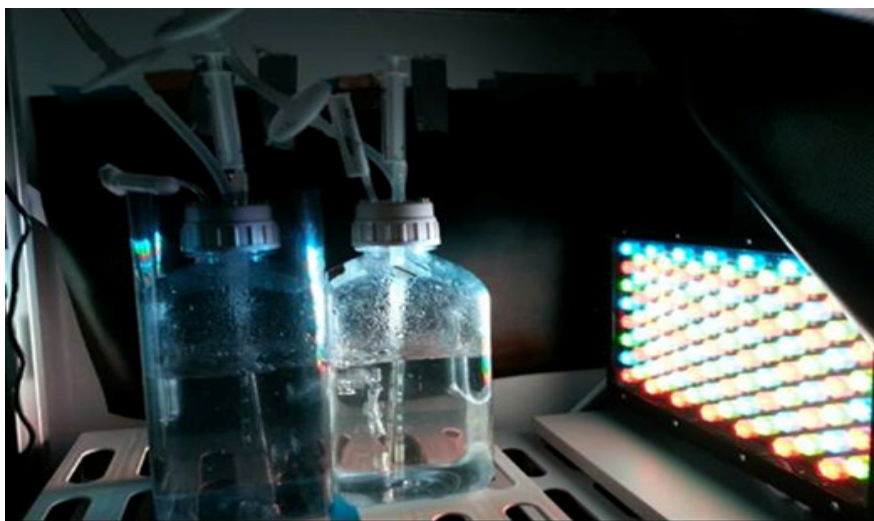


Figure 11. Instrumental set up for Experiment 2

4.3 Sampling

Each bottle was sampled every morning at 9:00-10:30 am 10 ml sample was taken in a 20 ml clean, liquid scintillation counting (LSC) vials from each of the bottles with a 10ml syringe placed in the bottle cap. The collected samples were covered most of the times to prevent their reaction with light or foreign particles.

4.3.1 Monitoring growth

Cell growth was monitored daily (excluding weekends) using a FlowCAM particle analyzer (Fluid Imaging technologies, Inc., USA). The FlowCAM system uses a pump (peristaltic, syringe or vacuum) to pull the fluid sample through a flow cell perpendicular to the optical path. The optical system is similar to that of the microscope, and is used to capture the real time images of the particles in the fluid as they pass through the flow cell. It typically takes 10,000 images/ minute. For each overall image captured the individual particles are extracted as separate small images and stored separately with over 30 individual particle measurements for each image.

The cell count was done twice and the average was taken as a final observation result. The recorded cell count number was then used to simulate the number of cells for rest of the week using following growth equation:

$$K' = \frac{\ln\left(\frac{N_2}{N_1}\right)}{T_2 - T_1} \quad (3)$$

Where, K' = growth rate, N_1 and N_2 are biomass at Time 1 (T_1) and Time 2 (T_2) respectively.

The logarithmic growth equation was used to simulate the algae growth for rest of the week in Excel 2010. Dilution was done when needed. Moreover, in this study inevitable affects such as self-shading and photoinhibition were minimized as much as possible. To avoid self-shading, the samples were diluted when needed and the cell counts were limited up to 500,000 cells /l.

4.3.2 Measurement of photosynthetic parameters using aqua pen

The photosynthetic parameters in the samples were measured by using AquaPen-C-AP-C100 (Photons Systems Instruments, spol.s.r.o). Aqua pen is equipped with a blue and red LED emitter, optically filtered and precisely focused to deliver light intensities up to 3,000 $\mu\text{mol (photon).m}^{-2}.\text{s}^{-1}$ to measured algal suspensions. The blue excitation light (455nm) is used mainly for chlorophyll excitation i.e. for measuring chlorophyll fluorescence in algal cultures. The Chlorophyll Fluorescence Induction Kinetics (OJIP), LC_1 (Light curve 1), LC_2 (Light curve 2), and Quantum yield (QY) were measured in each experiments.

The samples were first transferred to the 10mm Hellma cuvette, and placed in the Aqua Pen and connected to the computer. The obtained data is the processed in Excel.

4.3.3 Nile Red staining

Nile Red is a lipophilic stain which is prepared by boiling a solution of Nile blue with sulphuric acid. Nile Red in combination with DMSO (Di-methyl sulfoxide) penetrates the cell membranes and, in lipid-rich environment it emits the intense fluorescence which

can be measured using a spectrofluorometer. The fluorescence measurement in this experiment was done using Varian Cary Eclipse Spectrofluorometer to follow up the lipid accumulation. The fluorescence is linearly correlated with increase in the total lipid content (Sheehan et.al 1998, 54); however, it should be kept in mind that this method of lipid measurement does not quantify the total lipid content (Natunen, 2012).

A working solution of Nile Red in acetone (0.25mg/l) was used for the measurements. The cell wall penetration of the dye was enhanced by adding 0.3ml of DMSO (final concentration 10% (v/v)). The final concentration of Nile red in the samples was 1 μ g/l. The samples containing *P. tricornutum* each 3 ml were measured after adding 12 μ l of NR and incubating for 10 min. A blank measurement was carried out using Milli-Q (MQ) water. The fluorescence of the samples after Nile red staining was measured using a spectrofluorometer at certain settings (see Table 3) where Nile Red at certain wavelength reaches the excitation peak and emits the fluorescence.

4.3.4 Chla fluorescence measurement

The Chla pigment has a very useful property that a proportion of absorbed light energy is remitted with longer wavelength emission as fluorescence. Chla fluorescence can be measured in living cells (*in-vivo*) or after extraction of pigments from a solvent (Robert A.A, 2005). The Chla fluorescence measurement was carried out using a Varian Cary Eclipse spectrofluorometer (10mm, Hellma cuvettes). Before the fluorescence measurements, the culture samples were dark acclimated for 20 minutes. The samples were diluted if necessary. A blank measurement was always carried out with MQ water and the final Chla fluorescence value was obtained by subtracting the blank fluorescence and by multiplying by the dilution factor.

4.3.5 Nile Red fluorescence Measurement

As explained in the section 4.3.3, Nile red fluorescence measurement was carried out using a Varian Cary Eclipse spectrofluorometer, (10mm, Hellma cuvettes) on the final day of sampling for each of the light levels. Nile Red penetrates the cell wall and emits fluorescence at certain excitation and emission wavelengths. All the samples were introduced at the Nile red excitation and emission region as shown in Table 3 below.

Table 3. Excitation emission settings for spectrofluorometer.

Excitation wave lengths	440–680 nm, slit 5 nm
Emission wave lengths	530–580 nm, slit 5nm
Emission wave lengths	560–610 nm
PMT detector Voltage	High

The Nile Red concentration, the staining time and wavelengths used were chosen based upon unpublished studies on Nile Red staining of *P. tricornutum* by Seppälä, Spilling and Tamminen. The 10% (v/v) DMSO concentration had previously been proven effective for enhancement of Nile Red fluorescence with *P. tricornutum* (Natunen, 2012).

The obtained data was processed in Excel 2010. The samples were done in replicates so that the desired level of accuracy was obtained. The final value of Nile red fluorescence was obtained by subtracting the blank Nile Red measurement (Fluorescence emitted after Nile Red stained) and the Chla fluorescence (i.e. auto fluorescence of diatom *P. tricornutum*) and multiplied by the dilution factor if any. The dilution was done if the sample was too dense before doing the Chla measurement.

4.3.6 Dry Weight filtration

Dry weight filtration was carried out on the final sampling day for all light levels. The filtration arrangement was done as shown in Figure 12. Samples were passed through Whatman Glass micro filters (GFC) 25 mm in diameter (Cat No 1825-025) in the units, and the sample yields i.e. biomass were collected in the filters. The filtration was done for dry weight measurement, each 50ml. The filters used in this experiment were beforehand washed, pre combusted (450°C, 4h, Nabertherm Program controller S19) overnight, and were weighted in the micro scale (Sartorius micro). The obtained filter samples were again dried in the oven at 80°C and weighed.

The dry weight content of the sample yield (biomass) was calculated by subtracting the weight of the filters without the biomass from the weight of the filters with the biomass and by dividing the result by the volume filtered through the unit i.e. 50 ml.

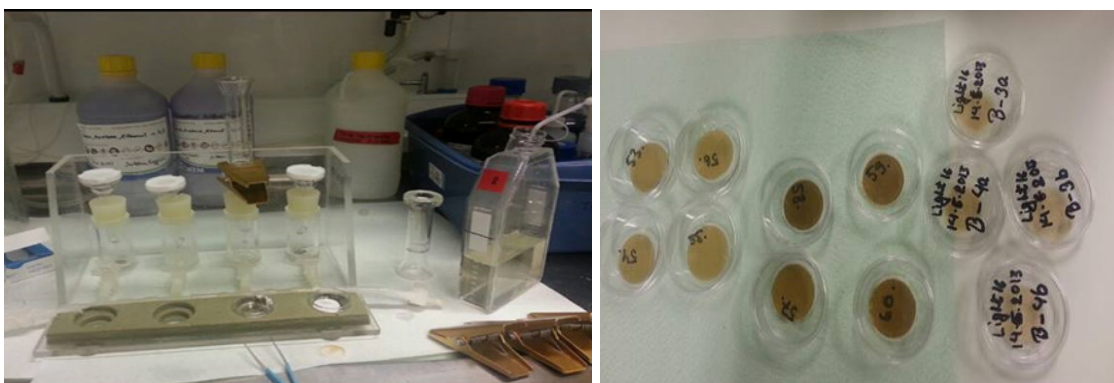


Figure 12. Filtration unit (a) and biomass samples on the filters (b).

In case, the filters could not be weighted immediately, the samples were stored at room temperature in a Petri dish as shown in Figure 12 (b).

4.3.7 Chlorophyll absorption spectra measurement

The culture samples (each 10ml) were filtered through the filtration unit as shown in Figure 10 on the sampling day. The biomass samples obtained were stored at -20°C in the freezer immediately after sampling. The chlorophyll absorption spectra were analyzed using Perkin Elmer Lambda 650 UV/VIS spectrophotometer. The obtained data was processed in Excel 2010.

4.3.8 Chlorophyll concentration measurement

The filters, immediately after measuring chlorophyll absorption spectra were transferred into LSC vials containing 10 ml of ethanol. A Varian Cary Eclipse Spectrofluorometer was used to measure the concentration of chlorophyll. The excitation and emission wave length used in this measurement were 430 nm and 670 nm wavelength with 5 nm wide slit respectively. The samples were transferred into a well plate with four standard Chla solutions at different concentrations i.e. 0.0092, 0.0459, 0.0917, 0.1376, 0.1834 Chla mg/l, respectively. Dilution was done if needed. A calibration curve was obtained with the standards with coefficient of determination ($R^2 = 0,997$). The Chla concentration data was processed in Excel 2010.

5 Statistical analysis

All statistical analyses were performed with Excel 2010 and R (R core Team 2012). To analyze the influence of irradiance and photo period in Experiment I, linear regression was done using R and contour plot was obtained. The nonlinear regression (nls) method in R was used to model growth irradiance curve using McIntyre (2002) equation. To investigate how the irradiance and photoperiod affect the chlorophyll and lipid content, a contour plot was made to investigate the influence of light period and irradiance on R. In addition, Excel 2010 was used to process the dry weight and chlorophyll data to simplify the data analysis. In the second results analysis, Excel 2010 was used for visualizing the growth data and a model of Nile Red per Dry Weight based on the exponential and stationary data was created and visualized using R (Statistics).

6 Results

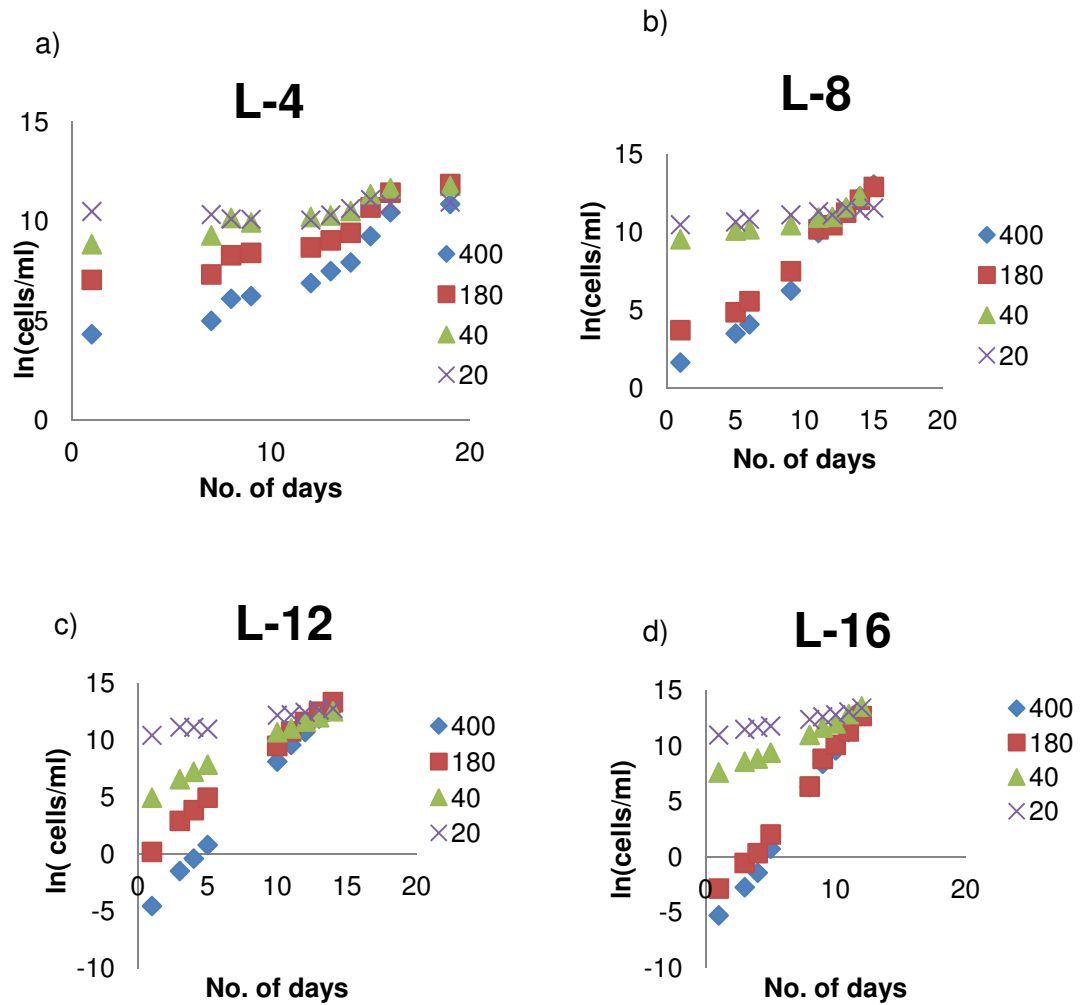
The results section presents measurement results and findings from the experiment 1 and experiment 2.

6.1 Experiment 1

To find out the effects of irradiance and photoperiod, the exponential growth data is first presented. Next, a least squares regression analysis was carried out to determine the growth rates for each photoperiod and irradiance levels. Furthermore, the growth irradiance curve is presented and the observed values are fitted using the Poisson function of MacIntyre et.al (2002). The curve fitting is done using nls (Nonlinear least squares) in R. Finally, a simple comparison is done using Chla/dry weight and Nile Red per dry weight measurement with respect to light dose. All the analyses have been made in duplicates during the experiment.

6.1.1 Exponential growth data

Figure 13 illustrates the exponential growth curves for all the photoperiods: L-4, L-8, L-12, L-16, L-20 and L-24, respectively. The x-axis represents the sampling/experimental days and y-axis represents the natural logarithmic cell numbers per ml. The four different symbols represent the different light irradiance levels.



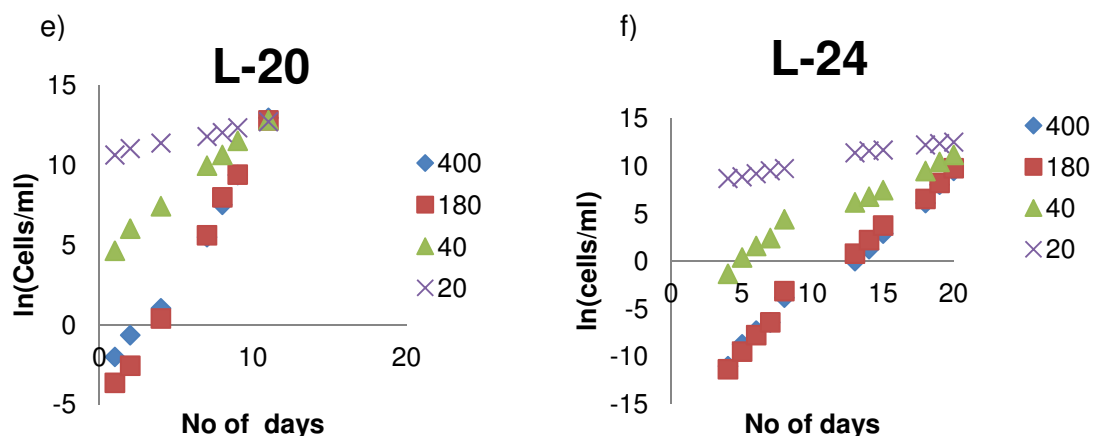


Figure 13. Graph (a) (b) (c) (d) (e) (f) Exponential growth curve for photoperiods and 4,8,12,16,20,24 h at irradiances each 400, 150, 40, 20 $\mu\text{mol}\cdot\text{q}\cdot\text{m}^{-2}\cdot\text{s}^{-1}$ irradiances.

A least squares regression analysis was carried out to find the growth rates which are listed in Table 4. The standard error for growth estimates and coefficient of determination (R^2) values for regression is also shown.

Table 4. Calculated growth rates using least square regression analysis at irradiances 400,180, 40 and 20 $\mu\text{mol}\cdot\text{q}\cdot\text{m}^{-2}\cdot\text{s}^{-1}$ and photoperiod 4, 8,12,16,20, and 24 h.

Note: Data points are taken from the last sampling week.

Photoperiod (L) (h)	Irradiances (I) ($\mu\text{mol}\cdot\text{q}\cdot\text{m}^{-2}\cdot\text{s}^{-1}$)	growth rate (d^{-1})	Standard error	Coefficient of determination (R^2)
4	400	0.405	0.247	0.980
4	180	0.325	0.021	0.995
4	40	0.138	0.004	0.999
4	20	0.076	0.047	0.328
8	400	0.772	0.008	1.000
8	180	0.706	0.065	0.975
8	40	0.544	0.076	0.945
8	20	0.073	0.052	0.393
12	400	1.137	0.069	0.989
12	180	0.940	0.046	0.993
12	40	0.466	0.022	0.993
12	20	0.160	0.016	0.969

Photoperiod (L) (h)	Irradiances (I) ($\mu\text{mol}\cdot\text{q}\cdot\text{m}^{-2}\cdot\text{s}^{-1}$)	Growth rate (d^{-1})	Standard error	Coefficient of determination (R^2)
16	400	1.568	0.069	0.994
16	180	1.516	0.139	0.975
16	40	0.632	0.041	0.988
16	20	0.250	0.016	0.987
20	400	1.858	0.037	0.999
20	180	1.754	0.108	0.992
20	40	0.717	0.031	0.996
20	20	0.232	0.016	0.990
24	400	1.694	0.048	0.998
24	180	1.667	0.065	0.995
24	40	0.884	0.020	0.998
24	20	0.161	0.007	0.994

Table 4 shows the growth rates at different photoperiod and irradiances. The highest growth rate i.e. $1.85 (\text{d}^{-1})$ was observed at a photoperiod of 20 h at irradiance level of $400 \mu\text{mol}\cdot\text{q}\cdot\text{m}^{-2}\cdot\text{s}^{-1}$ while the lowest growth rate i.e. $0.07 (\text{d}^{-1})$ was observed at photoperiod of 4 h at irradiance $20 \mu\text{mol}\cdot\text{q}\cdot\text{m}^{-2}\cdot\text{s}^{-1}$. Moreover, the R^2 values in most cases are < 0.95 except for light condition L-4 and L-8 at irradiance of $20 \mu\text{mol}\cdot\text{q}\cdot\text{m}^{-2}\cdot\text{s}^{-1}$. The least value of R^2 can be explained by the limitation of light. Table 4 in general shows that the growth rate was higher at high light and longer photoperiod, while the growth rate was lower at lower light condition. To visualize the effect of irradiance and photoperiod in *P. tricornutum*, a contour plot was made which is briefly discussed below.

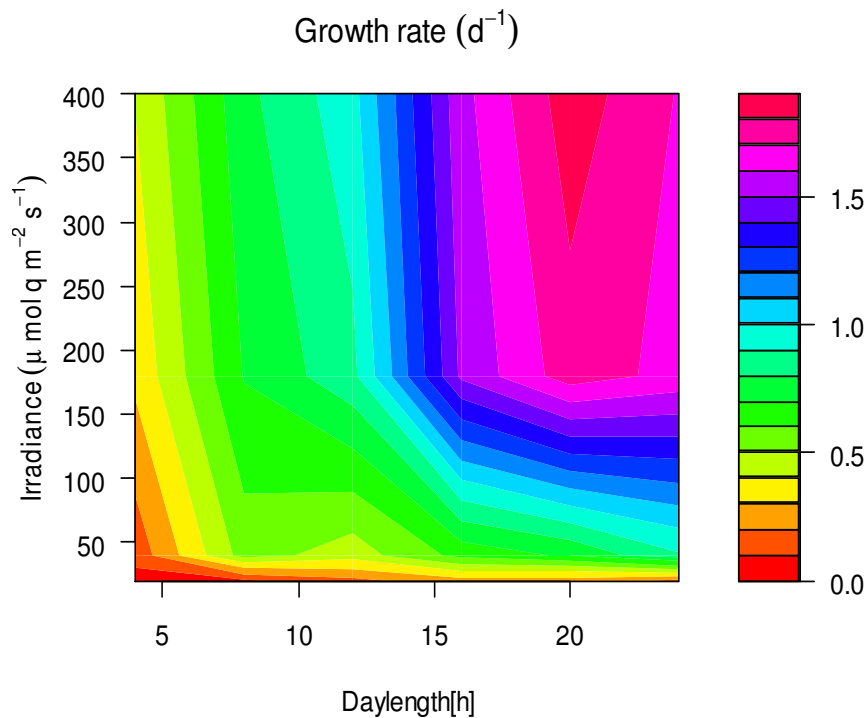


Figure 14. Contour plot of the growth rates with respect to irradiance and photoperiods

The influence of photoperiod on growth rates at varying irradiances is shown in the contour plot in Figure 14. The growth rates are higher at longer photoperiods or day length and at higher irradiances, while the lowest growth rates are observed at low irradiance and shorter photoperiods. It also shows that even at the same irradiance, when moving from a shorter day length to a longer day length, the growth rates are higher at longer photoperiod than shorter photoperiod. A maximum growth rate can be seen at photoperiod 20h while the least at 4h. A slight decline in growth rate was observed at light period 24h which could be due to excess light condition also called photoinhibition. In summary, the influence of irradiance and photoperiod on growth rates of *P. tricornutum* can be seen as dynamic.

6.1.2 Growth-Irradiance curves

Growth-irradiance curves are used to predict the growth rates under different irradiances and photoperiods. By determining which factors are mainly responsible for the variability in growth, it is possible to predict growth irradiance curves with more accuracy even from few measurement points. MacIntyre growth-irradiance equation (2002) shown in Equation 4 is used to model the growth-irradiance relationship in this study.

The equation consists of μ as observed growth rates, μ_{\max} as maximum growth rates, growth saturation parameter (Ke) and Irradiance level (I). Only observed growth rates (μ) and Irradiance (I) are known in this case. To find out the two remaining unknown parameters, a nonlinear least squares (NLS) method can be used to fit the model for all light levels.

$$\mu = \mu_{\max} \left(1 - \exp \left(-\frac{I}{Ke} \right) \right) \quad (4)$$

Where, μ = observed growth rate (d^{-1}), μ_{\max} = Maximum growth rate (d^{-1}), I = irradiance level ($\mu\text{mol}\cdot\text{q}\cdot\text{m}^{-2}\cdot\text{s}^{-1}$), Ke = Growth saturation parameter ($\mu\text{mol}\cdot\text{q}\cdot\text{m}^{-2}\cdot\text{s}^{-1}$)

The main objective in NLS is to fit a nonlinear model with two unknown values which in this case was the maximum growth rate (μ_{\max}) and growth saturation parameter (Ke). The residual sum of squares in the NLS summary provides the best indication of the distance between observed and predicted values (the lower is the distance, the better is the fit). Table 5 shows the values calculated for the growth saturation parameter (Ke) and maximum growth rates (Ke) using Equation 4.

Table 5. Specific growth rates and growth saturation parameter values obtained from nonlinear regression in R.

Photo period (h)	Maximum growth rates (μ_{\max})	Growth saturation parameter (Ke)	Residual std error
4	0.43	129.88	0.045
8	0.81	109.00	0.061
12	1.14	92.667	0.074
16	1.63	83.27	0.934
20	1.82	88.80	0.131
24	1.75	72.09	0.217

Using the values for maximum growth rates (μ_{\max}) and growth saturation parameter (Ke) obtained from the Nonlinear Regression, model plots were made in R as shown in Figure 15.

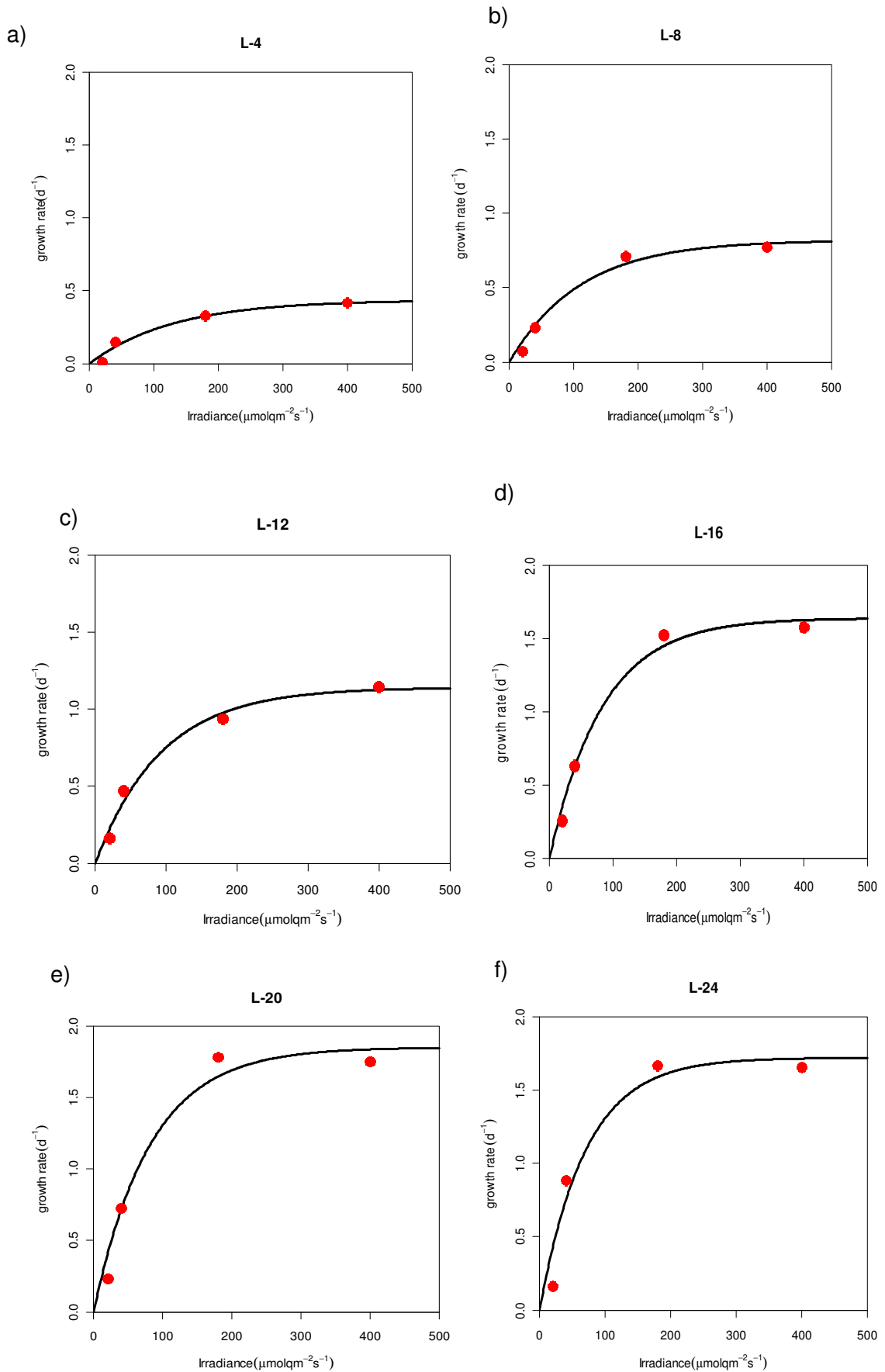


Figure 15. Growth irradiance curve based on the observation values and fitted values (a) L-4, (b) L-8, (c) L-12, (d) L-16, (e) L-20 and, (f) L-24. Solid black curve in the graph represents the fitted model. The red dots represent the measured (observed) growth rates in each of the graphs. The x- axis represents the irradiance level while the y-axis represents the maximum growth rates.

The results of the fitted data using the Poisson function of MacIntyre equation is seen in the graphs (a) (b) (c) (d) (e) and (f) for each photoperiod named as L-4, L-8, L-12, L-16, L-20, and L-24, respectively. The growth rate of the cells in each light condition increased with increasing irradiance and photoperiod in each case until they reached the maximum value which is also called specific growth rate or maximum growth rate (μ_{max}). The growth rate is maximal when the algae are light saturated. Beyond this saturated irradiance level the specific growth rate (μ_{max}) had no significant effects on the growth for all the light condition. The nature of curve is also seen different in each light condition.

Furthermore, the photo period and the growth saturation parameter (Ke) obtained from the growth- irradiance model were plotted to see the independent effects of photo period h on the specific growth rate of the cells in Figure 16.

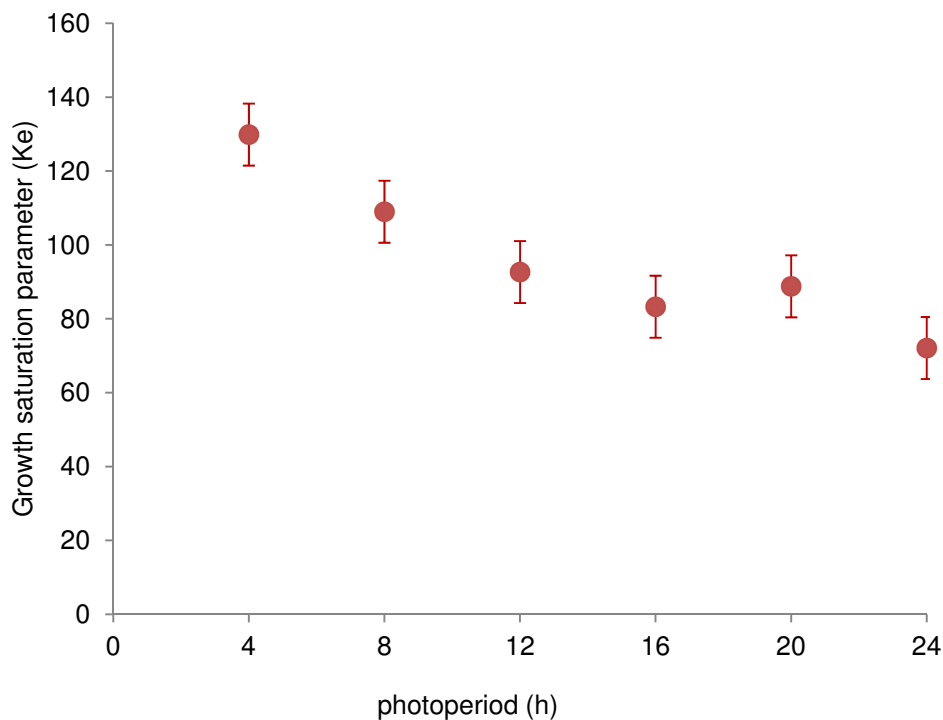


Figure 16. Photoperiod vs. growth saturation parameter (Ke).

Figure 16 shows the relationship between the photoperiod and the growth saturation parameter (K_e) is a decreasing linear trend. The growth saturation parameter when moving from shorter photoperiod shows a decreasing trend that slows down at higher photoperiods. It looks that the cells at shorter photoperiods require higher amount of light or irradiance to get light saturated and vice versa. A slight rise is observed at photoperiod 20 h and a decrease at photoperiod 24 h. However, the error bars shows the increase not very significant. Similarly, Figure 17 illustrates the relationship between the maximum growth rates (μ_{max}) at varying photoperiods.

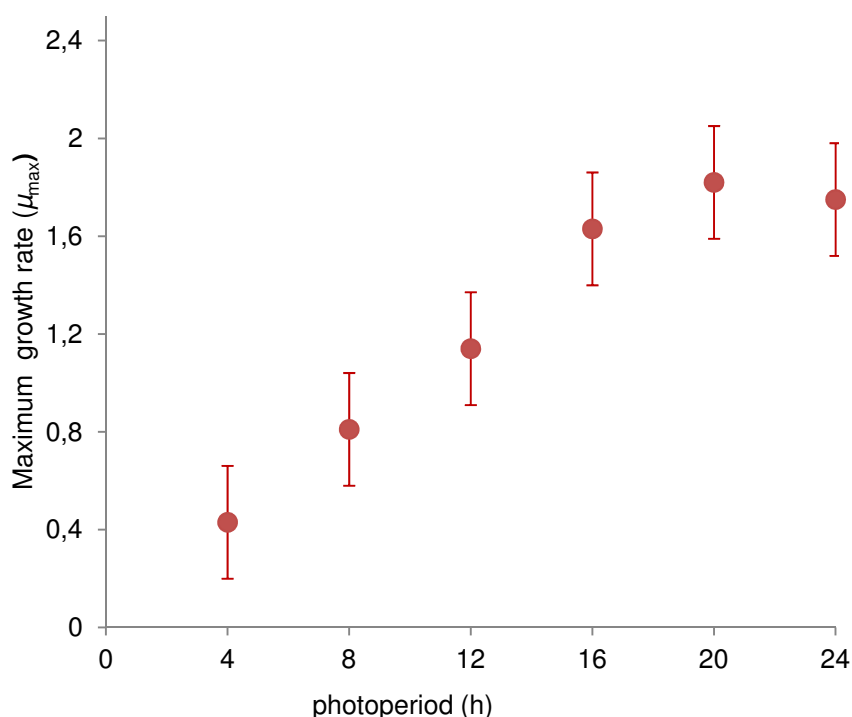


Figure 17. Photoperiod vs. maximum growth rate

The relationship between the photo periods vs. specific growth rates seems to be a concave-shaped increasing trend. The cells at longer photo periods show higher growth rates than the ones at shorter photo periods. The growth rate rises significantly up from photoperiod 4 h to 20 h and slowly declines at photo period 24 h. From the figure, it is clear that if the light exposure time or photoperiod decreases, irradiance alone is not very effective to enhance the growth rates in the cells. The figure also supports the phenomena of photo inhibition, in which the algae cells become photo stressed and the growth rate decreases.

6.1.3 Chla vs. dry weight measurement

To understand the algae light dependency and chlorophyll synthesis mechanics related to growth rate the light integration or light dose $\text{mol}\cdot\text{q}\cdot\text{m}^{-2}\cdot\text{d}^{-1}$ was calculated by multiplying the irradiance with photo period. The results are illustrated in Figure 18.

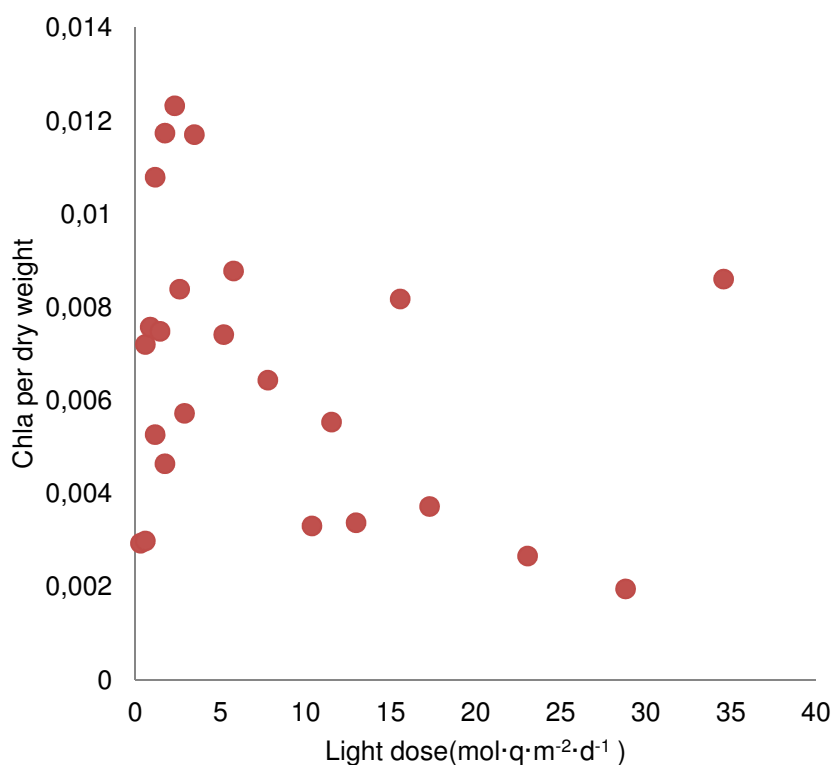


Figure 18. Chlorophyll per dry weight vs. the light dose.

Figure 18, illustrates the chlorophyll per dry weight values of *P. tricornutum* at different light doses. The maximum chlorophyll content per biomass 0.0123 (mg/mg) was obtained at lower light dose of $2.34 \text{ mol}\cdot\text{q}\cdot\text{m}^{-2}\cdot\text{d}^{-1}$ and the minimum Chla per biomass 0.0019 (mg/mg) at higher light dose of $28.8 \text{ mol}\cdot\text{q}\cdot\text{m}^{-2}\cdot\text{d}^{-1}$. Although, a general decreasing trend of Chla content (as in MacIntyre 2002) can be seen when moving from lower light doses to higher light doses, two unexpected Chla per dry weight values are also seen at light dose of 15.52 and 34.56 $\text{mol}\cdot\text{q}\cdot\text{m}^{-2}\cdot\text{d}^{-1}$, respectively. These two points can be a random behavior shown by the species or an experimental error. Moreover, a contour plot was made in R to show the dependency of chlorophyll content with respect to the photoperiods and the irradiances.

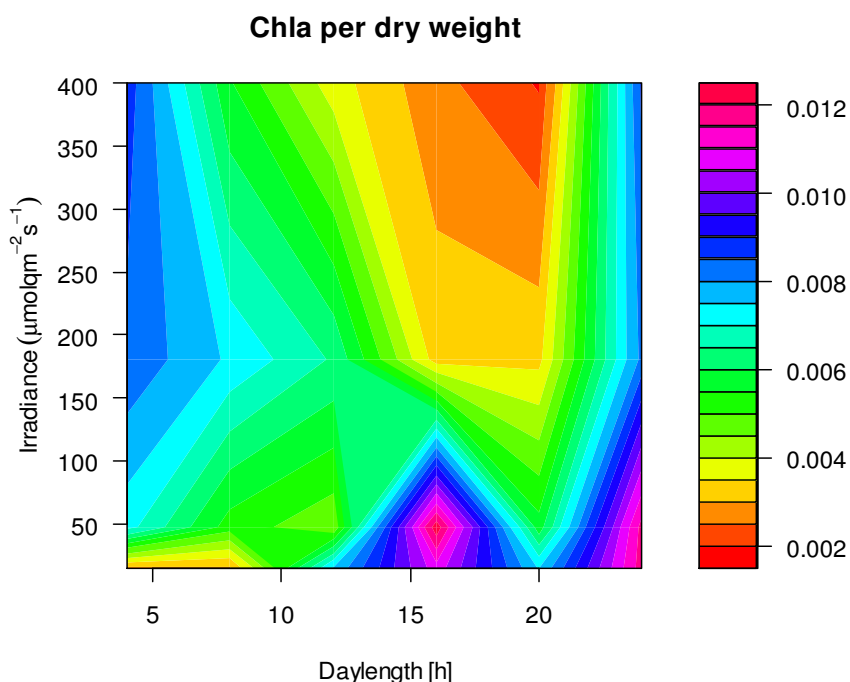


Figure 19. Contour plot for Chla per dry weight.

Figure 19 shows the areas with higher irradiances and longer photoperiods are amongst the ones with lowest chlorophyll content. On the contrary, the areas with lower irradiance and shorter photo period have somewhat higher chlorophyll content than the ones with higher irradiances and shorter photo periods. A maximum rise in the chlorophyll content was observed at lower irradiance and longer photoperiod i.e. at 16 h and 24 h. The slightly higher concentration in high irradiance areas is a suspect if it is due to photoinhibition or an experimental error.

6.1.4 Nile Red vs. dry weight measurement

Nile Red fluorescence per dry weight values were plotted to see if there is any correlation between the changing irradiances, photoperiods and lipid content. A very good example of correlation was observed at photoperiod 20 h which is presented in Figure 19.

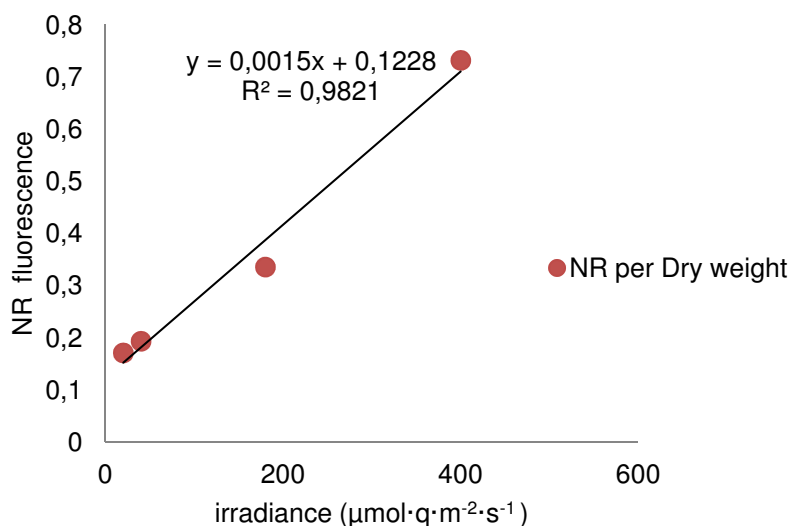


Figure 20. Nile red fluorescence vs. dry weight at photo period 20 h.

Figure 20 strongly suggests a rise in NR fluorescence per dry weight values with respect to the irradiances at photoperiod 20 h. The maximum amount of NR fluorescence was obtained was 0.7 NR per dry weight at an irradiance of $400 \mu\text{mol}\cdot\text{q}\cdot\text{m}^{-2}\cdot\text{s}^{-1}$ while, the least was between 0.1 to 0.2 NR per dry weight at lower irradiances of 40 and 20 respectively. The coefficient of determination R^2 value also suggests that the model fits well. Hence, the relation is linear. A contour was plotted in R to compare the changes in lipid content with respect to the photoperiods and Irradiances at the exponential phase. The contour plot is as shown in the Figure 19.

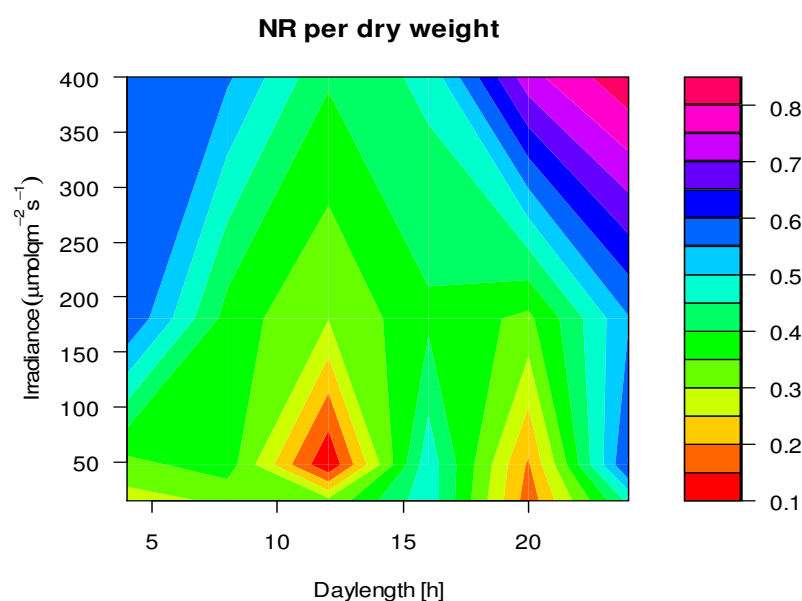


Figure 21. Contour plot for NR fluorescence per dry weight.

The contour plot shows the Nile red per dry weight was found to be the highest in the areas with higher irradiances and longer photoperiods. And the lowest Nile red per dry weight was found at the areas with lower irradiances and shorter photoperiods. In the contour, two significant areas at photoperiods 12 and 20 h were also observed to have very low NR fluorescence values. The very low concentration could be due to light limitation due to self-shading or an experimental error. To understand the correlation in detail, the NR fluorescence per dry weight can be plotted against the light dose as shown in Figure 22.

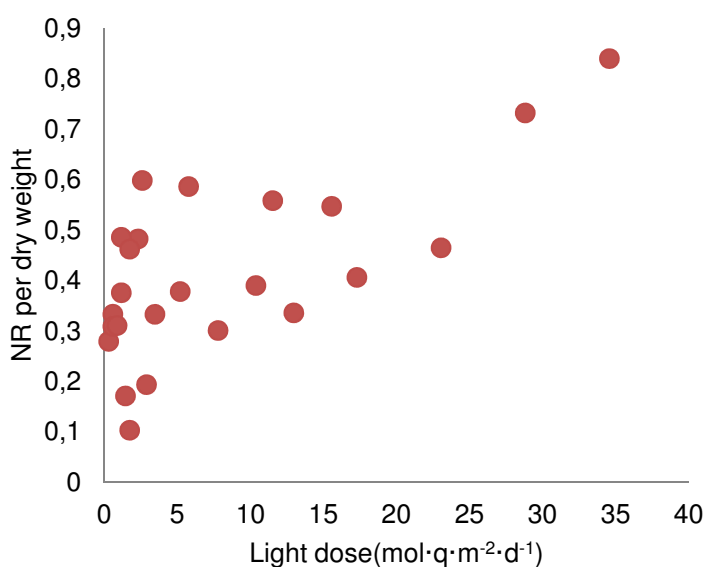


Figure 22. NR per Dry weight vs. the light dose.

Figure 22 illustrates the values of NR per dry weight with respect to the changing light doses. The maximum NR per dry weight value is seen at light dose of 34.56 mol·q·m⁻²·d⁻¹ and the minimum at 1.78 mol·q·m⁻²·d⁻¹. In addition, the NR per dry weight values remained randomly dense at the lower light doses ranging from 0 till 16 mol·q·m⁻²·d⁻¹ and started to increase significantly from 0.4 to 0.8 (NR per DW) as the light dose increased from 23 till 34 mol·q·m⁻²·d⁻¹.

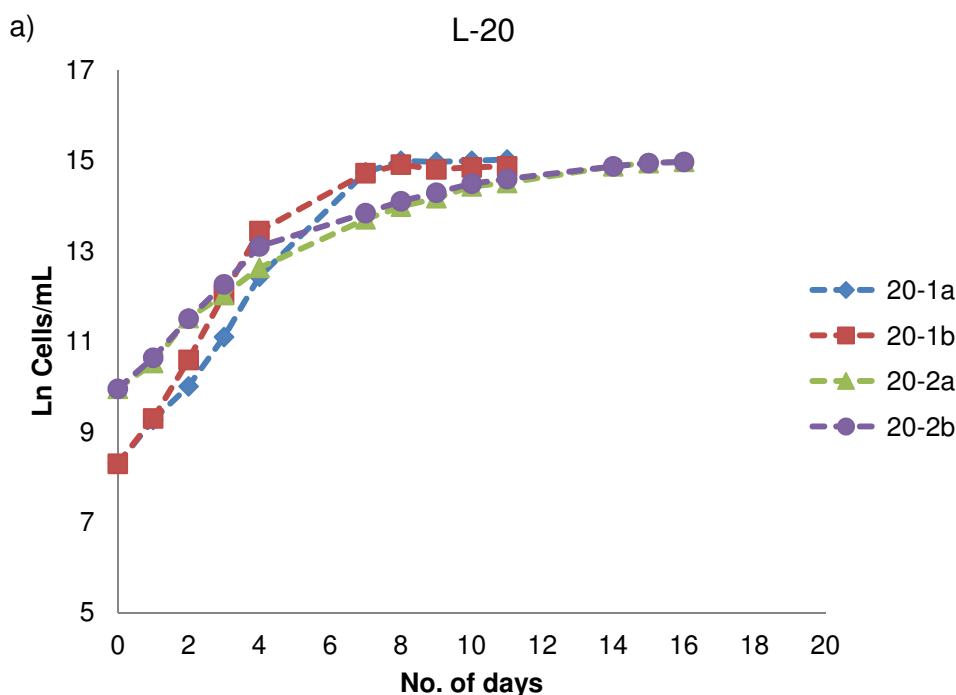
The plot suggests that the higher the light dose is, the more NR fluorescence per biomass produced is and vice-versa. It looks that the light dose does affect the accumulation of lipids, but the behavior is more or less random at lower light doses.

6.2 Experiment 2

The growth curve is first considered. And a detailed comparison of Nile Red / dry weight is done to find out the variation on lipid content with respect to the experimental days. Finally, results from 2^2 factorial experiment for daily lipid accumulation is discussed and a model of NR per DW as a function of day length and irradiance is made. The model is then visualized as a contour plot with the measured values and the outcome of the model is discussed.

6.2.1 Growth Monitoring

In this experiment, the cell count was done using flowCAM and a natural logarithmic of the cell numbers was calculated using the growth equation. Figure 21 shows the growth of algae cells from the exponential to the stationary phase from day 1 to the sampling day. The cells were grown in nitrogen-deficient medium thus, making favorable environment for lipid accumulation in the cells. The x-axis shows the number of sampling days and the y-axis shows the natural logarithmic number of cells per ml. The cell count was done in duplicates for each measurement and the average is taken to minimize the experimental error.



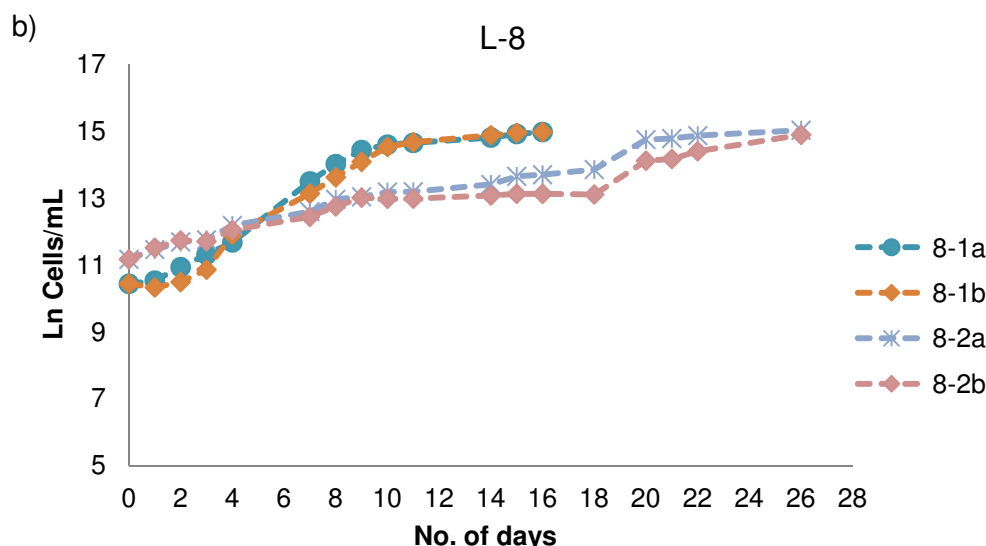


Figure 23. Growth curves at the stationary phase (a) L-20 and (b) for L-8 photoperiod. Note: 1a and 1b are the replicates of culture grown at irradiance $180 \mu\text{mol}\cdot\text{q}\cdot\text{m}^{-2}\cdot\text{s}^{-1}$ and 2a and 2b are replicates of the culture grown at irradiance of $72 \mu\text{mol}\cdot\text{q}\cdot\text{m}^{-2}\cdot\text{s}^{-1}$.

Growth measurement plot 23 (a) and (b) shows that the logarithmic growth of cells at stationary phases at two different photoperiod 20 and 8 h respectively. In plot (a), the number of cells increased significantly from day 0 until day 5th however, after that the number of cells remained more or less constant leading to stationary phase. The cell growth was slightly slower in Figure 22 (b) compared to Figure 22 (a); nevertheless, it also reached the stationary phase after 9th day. The growth of the cells of the second samples 8-2a and 8-2b slightly lagged in the beginning, which could be due to light limitation. After the cells reached the stationary phase growth, lipid monitoring was done daily. This phase provides the best environment for lipid accumulation. And this outcome is further discussed in the section 6.2.2 below.

6.2.2 Nile Red fluorescence measurement

Nile Red fluorescence measurement was done for both light levels, i.e. 20 and 8, every day. The natural logarithms of NR values were calculated using In function of the observed NR values in Excel 2010. Figure 24 shows the logarithmic value of Nile Red per day for photoperiod 20 and 8, respectively.

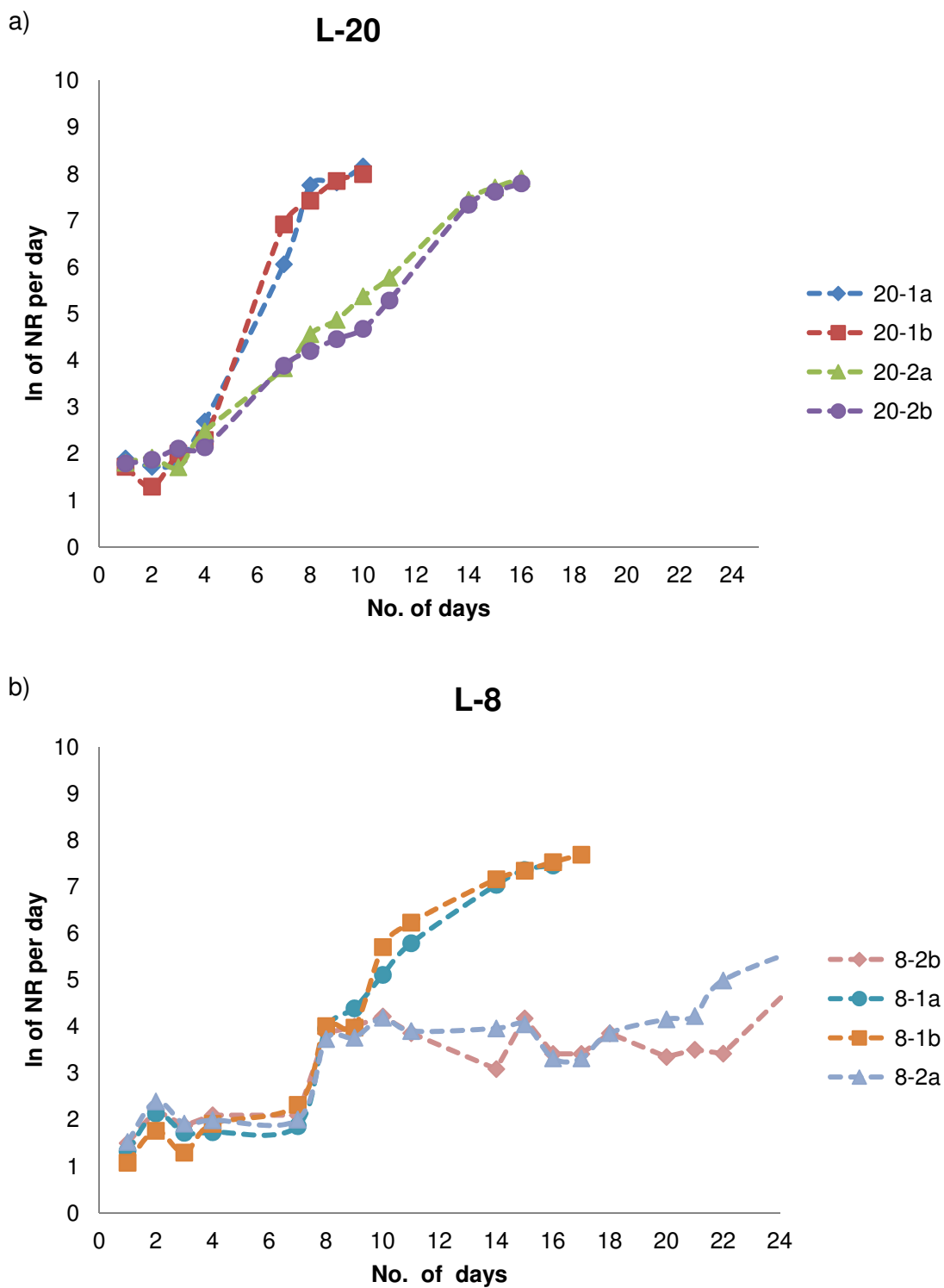


Figure 24. Log of NR per day for (a) L-20 and (b) L-8. Note: 1a and 1b are the replicates of culture grown at irradiance $180 \mu\text{mol}\cdot\text{q}\cdot\text{m}^{-2}\cdot\text{s}^{-1}$ and 2a and 2b are replicates of the culture grown at irradiance of $72 \mu\text{mol}\cdot\text{q}\cdot\text{m}^{-2}\cdot\text{s}^{-1}$.

The significant rise in total lipid content in both of the samples was observed in Figure 24 a. The lag phase lasted for 3 days and the increase in lipid content rose from day 4 until the final sampling day. Similarly, Figure 24 b also showed change in lipid content per day for both samples 8-1 and 8-2 at light condition 180 and 72 $\mu\text{mol}\cdot\text{q}\cdot\text{m}^{-2}\cdot\text{s}^{-1}$, respectively. The variation mainly started at day 7 for L-8. However, the 2nd sample of photoperiod 8h, 8-2a and 8-2b did not seem to perform very well due to low light availability. Compared to the lipid growth curves at Figure 24 (a), Figure 24 (b) showed a small lag phase in the beginning which could be due to the limitation of light. In spite of the lag phase in the beginning, the lipid content highly increased from day 8 to 11 and slowly saturated from day 11 till day 17. In order to analyze the rate of increase in total lipids per day, the slopes of the NR were calculated.

Table 6. Rate of increase in lipids per day.

Samples	Slope	Coefficient of determination (R^2)
20-1a	0.000234	0.902
20-1b	0.000205	0.950
20-2a	0.000124	0.976
20-2b	0.000134	0.996
8-1a	0.000085	0.984
8-1b	0.000068	0.989
8-2a	0.000016	0.978
8-2b	0.000004	0.775

The coefficient of determination values for all the samples was > 90 except for sample 8-2b which is due to low light condition and self -shading. The logs of NR values in Table 6 are taken from the last sampling week.

The bar chart in Figure 25 shows the rate of NR increase per day at the stationary phase at photoperiod of 20 h and 8 h. The two blue bars represent the light period 20 h and the two red bars represent the light period 8 h. The legends 20-1 and 20-2 represent the irradiance level of 180 and 72 $\mu\text{mol}\cdot\text{q}\cdot\text{m}^{-2}\cdot\text{s}^{-1}$ respectively, at photoperiod of 20 h. Similarly, 8-1 and 8-2 represents the irradiance level of 180 and 72 $\mu\text{mol}\cdot\text{q}\cdot\text{m}^{-2}\cdot\text{s}^{-1}$ respectively at a photoperiod of 8 h. The values shown in the bar graph is the average

of the replicates. As, seen from Figure 25, the rate of NR per day is highest at 20-1 and at its lowest at 8-2 samples. The difference in rate of increase can be explained by the different photoperiods. Moreover, when comparing the samples at same photoperiod but different irradiances, a huge variation in the NR values can be seen. In summary, the variation of lipid content with respect to irradiances and photoperiod is very distinct.

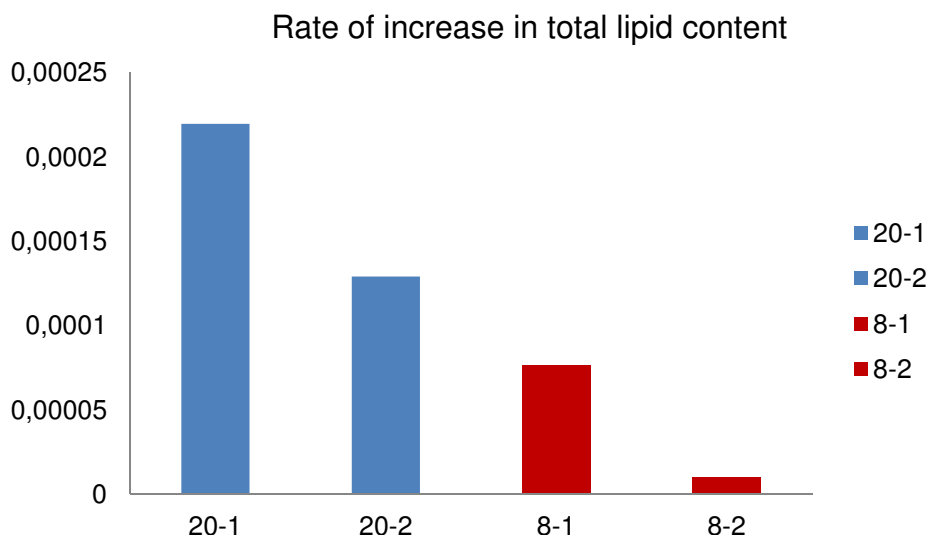


Figure 25. Rate of increase in NR per day. 20-1 and 20-2 represents the irradiance level of 180 and $72 \mu\text{mol}\cdot\text{q}\cdot\text{m}^{-2}\cdot\text{s}^{-1}$ respectively at photoperiod of 20 h. 8-1 and 8-2 represents the irradiance level of 180 and $72 \mu\text{mol}\cdot\text{q}\cdot\text{m}^{-2}\cdot\text{s}^{-1}$ respectively at photoperiod of 8 h.

6.2.3 Lipid Growth Model

Using the Nile Red fluorescence data, a lipid growth model can be obtained. The lipid growth model was made in R. The design matrix used in the model is shown in Table 6. The design variables were day length (L), irradiance (I) and time (t). Day length and Irradiance were the explanatory variable while NR per DW was the response variable.

Table 7. Data matrix of NR per DW values for Model 1 and Model 2. Time represents the sampling days, L represents the day length i.e. 8 and 20 h, t_p refers to the time point; t_1 and t_2 refers to time point 1 at exponential growth and time point 2 at stationary growth, I refers to the Irradiance 72 and $180 \mu\text{mol}\cdot\text{q}\cdot\text{m}^{-2}\cdot\text{s}^{-1}$ respectively and NR. Per DW means the Nile red fluorescence per Dry weight. Note: a and b are the replicates in each case!

Name	Replicates	Date	time	L	time point	I	NR per DW
Stationary_exp_L-20_1	a	16.8.2013	0	20	t1	180	0.300
Stationary_exp_L-20_1	b	16.8.2013	0	20	t1	180	0.196
Stationary_exp_L-20_1	a	23.8.2013	7	20	t2	180	22.17
Stationary_exp_L-20_1	b	23.8.2013	7	20	t2	180	16.61
Stationary_exp_L-20_2	a	16.8.2013	0	20	t1	72	0.342
Stationary_exp_L-20_2	b	16.8.2013	0	20	t1	72	0.169
Stationary_exp_L-20_2	a	29.8.2013	13	20	t2	72	14.68
Stationary_exp_L-20_2	b	29.8.2013	13	20	t2	72	13.83
Stationary_exp_L-8_1	a	19.8.2013	0	8	t1	180	0.105
Stationary_exp_L-8_1	b	19.8.2013	0	8	t1	180	0.107
Stationary_exp_L-8_1	a	29.8.2013	10	8	t2	180	13.43
Stationary_exp_L-8_1	b	29.8.2013	10	8	t2	180	12.64
Stationary_exp_L-8_2	a	19.8.2013	0	8	t1	72	0.19
Stationary_exp_L-8_2	b	19.8.2013	0	8	t1	72	0.224
Stationary_exp_L-8_2	a	9.9.2013	21	8	t2	72	2.55
Stationary_exp_L-8_2	b	9.9.2013	21	8	t2	72	2.28

Table 7, illustrates the NR per DW values at exponential and stationary phase at different time points (t_p) in the design matrix. The first sampling took place at starting of exponential phase and the 2nd sampling took place on the last sampling day at stationary phase. Time point 't₁' and 't₂' represents the time point at exponential growth and stationary growth respectively. Two models: 'Model1' and 'Model2' were created to denote the lipid growth model at time point 1 't₁' and time point 't₂' respectively. Both of the models were run in R. The effects were first analyzed by trial and error method. Only the models giving the most significant values were taken into account. The R output summary for both of the models is shown in Figure 26.

Figure 26. R output summary for Model 1 and Model 2 of lipid growth at exponential phase and stationary phase respectively. 'L' represents the photoperiod h and 'I' represents the irradiance $\mu\text{mol.q.m}^{-2}.\text{s}^{-1}$. NR per DW refers to the lipid numbers.

```
Call:
lm(formula = NR.per.DW ~ 1, data = my.Data, subset = tp == "t1")

Residuals:
    Min       1Q   Median       3Q      Max
-0.09925 -0.05106 -0.01023  0.03884  0.13749

Coefficients:
            Estimate Std. Error t value Pr(>|t|)
(Intercept)  0.20460    0.02969   6.892 0.000233 ***
---
Signif. codes:  0 '***' 0.001 '**' 0.01 '*' 0.05 '.' 0.1 ' ' 1

Residual standard error: 0.08397 on 7 degrees of freedom

Call:
lm(formula = NR.per.DW ~ L + I, data = my.Data, subset = tp ==
    "t2")

Residuals:
     3     4     7     8    11    12    15    16
1.4080 -4.1503  1.7976  0.9448  1.7682  0.9741 -1.2336 -1.5088

Coefficients:
            Estimate Std. Error t value Pr(>|t|)
(Intercept) -7.53119    3.04548  -2.473  0.05633 .
L             0.75853    0.14721   5.153  0.00361 **
I             0.07295    0.01636   4.460  0.00664 **
---
Signif. codes:  0 '***' 0.001 '**' 0.01 '*' 0.05 '.' 0.1 ' ' 1

Residual standard error: 2.498 on 5 degrees of freedom
Multiple R-squared:  0.9028,    Adjusted R-squared:  0.8639
F-statistic: 23.22 on 2 and 5 DF,  p-value: 0.002946
```

R summary output for model 1 did not show any significant effect on the lipid accumulation as the NR per DW values were < 1 and the values of L and I were not statistically significant. However, the R summary output for model 2 showed significant effects of day length 'L' and irradiance 'I' on the lipid accumulation per day. The obtained model from Model 2 is:

$$\text{NR Per DW} = -7.523119 + 0.75853 \times L + 0.07295 \times I + \text{error} \quad (5)$$

As mentioned previously, Model 1 did not show significant effects thus, gave a constant plane which was not worth plotting. This means, the L and I did not have any effects on the lipid accumulation in both light levels L-8 and L-20 at the exponential phase.

On the other hand, a well fitted contour plot of Model 2 was obtained as shown in Figure 27. The lipid content was higher at a longer day length i.e. 20 h than at day length 8 h at constant irradiance level of $72 \mu\text{mol}\cdot\text{q}\cdot\text{m}^{-2}\cdot\text{s}^{-1}$. The values differed by approx. 7 folds when moving from shorter day length to longer day length at the same irradiance. Similarly, the lipid content values changed from an average of 14 to 19.4 at higher irradiances. This shows that when moving from shorter day length i.e. 8h to a longer day length 20 h at constant irradiance of $180 \mu\text{mol}\cdot\text{q}\cdot\text{m}^{-2}\cdot\text{s}^{-1}$, the lipid content in *P. tricornutum* rose by approx.1.5 folds. The rate of change is more prominent when moving from a shorter day length to a longer day length at the lower irradiance than at higher irradiance. Furthermore, the p- value obtained from model 2 was < 0.005 and the values of L and I is significant as seen in the R summary in Figure 22. In addition, the obtained adjusted R- squared value is 0.8628 which also indicates the model fits well for a biological data as such. In summary, the effects of L and I on NR. Per. DW is seen significant at the stationary phase.

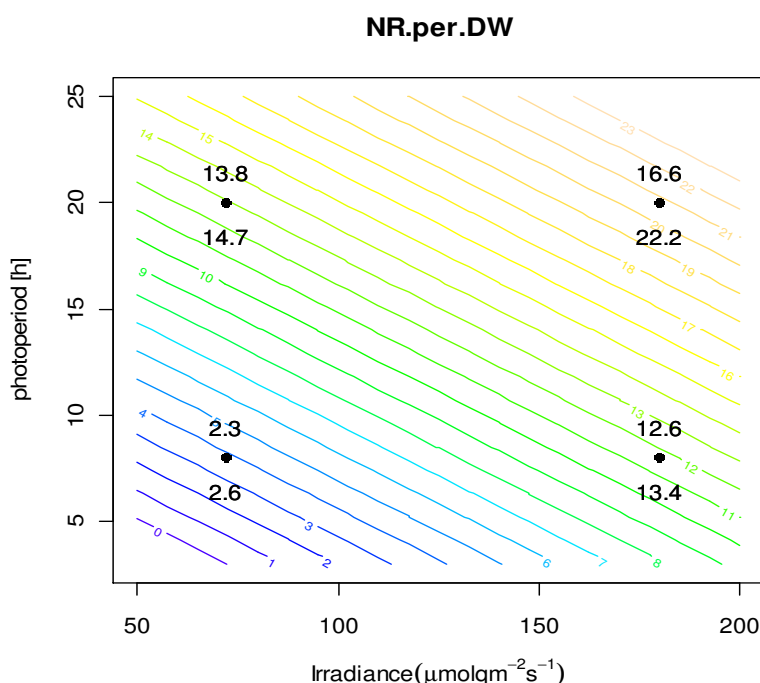


Figure 27. Contour plot of Model 2.

7 Discussion

This section highlights the effects of photoperiod and irradiance on growth rates and lipid contents, and limitations of the study.

7.1 Exponential phase growth data

The main goal in this experiment was to quantify the effects of photoperiod and irradiance on the growth rates of *P.tricornutum*. The experiment was done in nutrient replete condition so, that the only controlling factor was the light irradiance and photo period. The cell count was done using flowCAM and growth rate was calculated using the growth equation (See Equation 1).

The exponential phase growth data was plotted in Figure 13. The graph shows the exponential number of cells per day from day 1 till the sampling day. The sampling days were in longer interval for L-4 and L-24 due to several holidays but that did not really affect the growth rates. The dilution was done before hand to adjust the number of cells.

In addition, Table 4 showed very good values of coefficient of determination (R^2) of the measured growth rates for each photoperiod and irradiance level except for few of those which had R^2 values < 0.90 . The deviation was mainly observed at photo periods of 4 h and 8 h at lower irradiance level of $20 \mu\text{mol}\cdot\text{q}\cdot\text{m}^{-2}\cdot\text{s}^{-1}$. The cells in these conditions were lacking the amount of light due to shorter photoperiods and lower irradiance level arrangement, which consequently decreased the growth rates. In general, the linear regression analysis of the growth rates suggests good estimates of the measured growth rates.

7.2 Effect of photo period and irradiance on the growth of *P. tricornutum*

The contour plot Figure 14 suggests strong evidence on how the irradiance and the photo period affect the growth rates of *P. tricornutum*. The results suggested that even with the same amount of irradiance level the cells had lower growth at shorter photoperiod than at longer photoperiods. Hence, it is not only the irradiance that affects the growth rates but also the duration of light exposure to the cells. Similar behavior was

observed in the other photoperiods and irradiance levels. In high light condition, the cells received enough light to ease photosynthesis and hence, the cell growth. On the other hand, as the photoperiods and irradiance decreased it limited the amount of light energy to the cells which decreased the growth rates. Furthermore, a decrease in growth rate was observed at photo period 24 h which could be due to photoinhibition. At high light intensities, damage in the photosynthetic receptor system occurs, known as photoinhibition. If the cells received the light continuously it does not increase the rate of photosynthesis, rather it decreases, which eventually leads to decrease in the growth rates. This highlights the strong effects of effective light period and intensity on the growth rates of *P. tricornutum*.

Parmer et.al (2011) in their review article studied that light intensity and light period are the critical factors in determining the growth rate of microalgae in a phototrophic culture. It is because photosynthetic organisms like microalgae uses light as energy source to synthesize organic compounds which they use as energy storage or food. They also mentioned that if the microalgae are cultured at higher depth and cell concentrations, the light intensity must be increased to penetrate through the culture. Wahdin et.al (2013) also highlighted the effects of light intensity and photoperiod on the growth rate and lipid production of microalgae *Nannochloropsis sp.* in their experiment. The experiment included the treatment of the selected species for 9 days in three different light treatment mediums i.e. 50,100,200 $\mu\text{mol}\cdot\text{q}\cdot\text{m}^{-2}\cdot\text{s}^{-1}$ and three photoperiod cycles 24:0, 18:06 and 12:12 h at temperature 23 °C. A decrease in the growth rates of *Nannochloropsis sp.* was reported at light period 24 h which was discussed as photo inhibition. It appears that high light condition is not very favorable to achieve maximum growth rates in phototrophic microalgae species.

In summary, the growth of microalgae cells fully depends upon the amount of light absorbed and the efficiency with which the absorbed photons are converted into chemical energy by the photosynthetic reactions. Thus, the relationship between growth with combined effects of irradiance and photo period can be summarized as dynamic, i.e. the growth varies in response to varying light conditions. However, a phenomenon of photo inhibition is also obvious in phototrophic microalgae species like *P. tricornutum*.

7.3 Growth Irradiance Curve

A mechanistic growth model using Poisson function of MacIntyre (2002) was used to model the growth rates under different light conditions. The nls method was used in R to estimate the growth saturation parameter and maximum growth rate of *P. tricornutum*.

The growth irradiance model, in general showed a very good fit with small deviation of the observed values from the fitted values at higher light levels. Slight deviation of maximum growth rates were observed at photoperiods of 16, 20 and 24 respectively mainly at irradiances of $180 \mu\text{mol}\cdot\text{s}^{-1}\cdot\text{d}^{-1}$. The reason for the deviation could be the photo inhibition phenomenon which is not accounted in this model, but may play a role in higher photo periods. The reason why it was not taken into account was because solving the unknowns using four points of observation would not be statistically significant. Another down side of this model was that the intercept term (\propto^{Chla}) of growth curve was not taken into consideration. In many microalgae, the rate of light absorption is broadly correlated with the Chla-content (MacIntyre 2002). Moreover, the natures of the curves are also different at each light level. The reason for this could be that the light levels were different in each case, which affected the growth rates as discussed earlier.

To assess the independent effects of the photoperiods on the growth saturation parameter, the values obtained from the nls model were also plotted as shown in Figure 16. The relationship between photoperiod and K_e was seen almost linear. The shorter the photoperiod was the higher was the K_e and vice-versa. The main reason for this increase is that at shorter photoperiods, the cells require more light energy to maintain their growth rates, and hence, higher value of K_e was obtained.

The plot against specific growth rate (μ_{max}) and day length in Figure 17 shows an increasing trend from shorter photoperiods to longer photoperiods. The relationship between photoperiods and growth rates are similar for all light periods except for photoperiod 24 h, where a slight decrease in growth rate occurred due to photo inhibition as discussed earlier. Finally, when comparing both of the relationships there is inversely proportional correlation between photoperiod and growth rates; photoperiod and growth saturation parameter.

Algal growth models suggested by Laws and Bannister (1980) have assumed the relationship between maximum growth rate and photoperiod to be linear. A study on the causes of inter-specific variability in the growth irradiance relationship for phytoplankton by C. Langdon (1988) also highlights day length is important source of variability in maximum growth rate (μ_{max}). The difference between maximum growth rates from a long day to a short day can be 1 division (d^{-1}). Although, the situation can be complicated by the fact that the relationship between maximum growth rate and day length can follow several patterns in different species, maximum growth rate in most phytoplankton species has been observed to increase linearly on day length (Langdon 1988).

As reported in this thesis, *P. tricornutum* requires some hours of darkness to achieve the maximum growth rates. At extreme light condition, the algae cells can exhibit the photoinhibition that is fatal for photosynthetic apparatus and hence, decreases the growth rates. The growth performance of microalgae *P. tricornutum* is better at high light conditions however, with some period of darkness than at continuous high light. Thus, it should be kept in mind that while planning large scale cultivation and minimizing the production costs, it is more beneficial to identify the optimal light condition to maintain the productivity.

7.4 Effect of Photoperiod and Irradiance on Chlorophyll content

Chlorophyll, besides being a major photosynthetic pigment among phototrophic microalgae, is also widely recognized as a convenient correlative of biomass estimations of algae phytoplankton biomass and productivity. The total overview of the cellular composition of algae phytoplankton is complete only after examining the relationship between chlorophyll content and dry weight or volume (Reynolds 2006). Thus, similar measurement was carried out to assess the light utilization efficiency and productivity in this experiment.

The relationship of the Chla per dry weight was plotted with light dose in Figure 19. The figure revealed that the higher concentration of chlorophyll content at lower light doses and lower chlorophyll content at higher light dose. However, two unexpected point were also seen which can be described as an experimental error as it goes beyond the biological explanation. Another explanation could be that it is just a random behavior

shown by this species in photo stressed condition as the growth rate had also declined as discussed earlier. However, to make specific conclusions on the algae light dependency and chlorophyll synthesis mechanics still requires further studies and experiments.

Samuel et.al (1970) points out; the degree of light limitation is the primary controlling factor of chlorophyll synthesis during the phototrophic growth of micro- algae. The chlorophyll content increase when light is the limiting factor for growth under lower irradiances. With conditions, under which light is not a limiting factor for growth, photosynthetic reactions can proceed at greater rate than the photosynthetic products can be utilized. When the light becomes limiting, the excess photosynthetic products can be depleted. (Samuel et.al, 1970).

The contour plot supported a similar explanation to the hypothesis of lower chlorophyll content at high-light condition and higher chlorophyll content at the low-light condition. On the basis of the observation results, it can be said that the amount of light or the light conditions directly influences the chlorophyll synthesis in case of microalgae *P. tricornutum*. Hence, to maintain the highest biomass productivity it is necessary to have the cultures at optimum light conditions.

7.5 Effect of Photoperiod and Irradiance on Lipid content

Daily production of cell dry weight and amount of lipids could provide a decision making tool to assess biomass harvesting (Seppälä et.al, 2013). A linear relationship between lipid growth and irradiance level was observed at photoperiod 20h. The R^2 value of 0.98 also suggests the model as a good fit.

To assess the effects more in detail, a contour plot was made for NR fluorescence per dry weight at all photo period and irradiances. The contour, in general, showed the highest NR fluorescence at higher irradiance and longer photo periods and vice versa. However, it also showed high NR fluorescence at shorter photo period 4 h but at higher irradiances. In addition, a very low NR fluorescence at photo period 12 h and at 20 h, at the low irradiance region was observed. The reason could be that the cells had lower lipid content that gave a very low NR fluorescence value. Furthermore, the NR fluorescence remained changing when moving from photo period 8 h to 16 h. It appears that

the photo periods alone do not have significant effects on the lipid accumulation; rather, it is the combination of both irradiance and light period or the light dose at exponential growth phase. To examine the effects the same data was plotted with the light dose. The NR / dry weight values remained randomly dense at the lower light doses and started to increase significantly as the light dose increased.

The same conclusion can be drawn from this plot but it is hard to predict how the photo period affected the lipid growth at exponential growth. The effect is rather random for lower light dose, however; a significant trend is also seen at higher light doses. One possible explanation could be the random experimental error which is inevitable in such experiments. The NR blank also affects the NR fluorescence values which were observed different in each light condition and might have created random error in the final values. Another explanation might be that, the values of NR at the exponential phase can be very low or sometimes none at all, which could have given noisy values at lower irradiances at the exponential phase. As mentioned earlier, the best lipid growth is observed under nutrient stressed conditions. The stressed conditions are when the growth starts to slow down and the culture becomes nutrient limited. In experiment 1, the culture was only light limited so not clear increase or decrease was expected.

Nonetheless, it is clear in general that the light dose affects the lipid accumulation in *P. tricornutum*; however, no straight conclusions can be made how the lipid production differs with the photo periods at the exponential phase. To obtain high lipid productivity, the culture should be maintained at high light and nutrient limited conditions at the stationary phase.

7.6 Stationary phase growth data

The plots in Figure 23 a and 23 b showed the logarithmic growth of the cells at stationary phase. The algae cells achieve the stationary phase as the growth curve reaches the maximum plateau and flattens. When comparing both figures, the growth curve was seen much steeper at photoperiod 20 than at photoperiod 8 which can be explained by difference in the light levels. The cells receiving higher amount of irradiance at longer period divided more rapidly because the cells consumed free nitrogen quicker than the ones that received less amount of irradiance for shorter periods. Nevertheless, both of

the growth curves were followed slight lag in stationary phase in the beginning, mainly due to the nutrient exhaustion.

Furthermore, some limitations were encountered during the experiment essentially, due to the shading problems caused by increasing cell density in the adjacent bottles. The samples that received higher amount of light grew dense quicker and hindered the incoming light to the adjacent bottles. Therefore, the final sampling times are different for L-20 and L-8 samples. Samples 20-1a and 20-1b had to be sampled quicker. On the contrary, 8-2a and 8-2b had to be sampled later to examine their effects with respect to the day length and the irradiances. It was also trickier to define the exact sampling points due to the shading problems during the experiment. On the basis of the growth data, the samples were studied for lipid variation per experimental day.

7.7 Lipid Variation Per day

The main objective of this experimental part was to examine the change in lipid content per day of the microalgae species *P. tricornutum*. The cells were grown in nitrogen-limited media at light period of 20 h and 8 h at the stationary phase. The natural logarithmic values were plotted in Figure 24. The samples exposed to higher irradiance, i.e., $180 \mu\text{mol}\cdot\text{q}\cdot\text{m}^{-2}\cdot\text{s}^{-1}$ and longer day length 20 h performed very well and a clear rise in the total lipid content was seen. On the contrary, the samples exposed to lower light irradiance, i.e., $72 \mu\text{mol}\cdot\text{q}\cdot\text{m}^{-2}\cdot\text{s}^{-1}$ and shorter day length 8 h were seen to have slightly lower increase in the lipid content. The reason for this difference can be explained by the different light periods at the stationary phase, i.e. low light low lipids and high light high lipid productivity. During exponential growth, the cells use the organic carbon obtained from photosynthesis mainly for growth, however, at stationary phase when nutrient is limiting; the cells tend to accumulate lipids as energy storage compounds. In this case, as, the cell division slowed down, the culture became more and more nitrogen limited providing the best environment for lipid accumulation. Thus, a rapid increase in lipid was observed in the both of the graphs 24 a and 24 b.

Moreover, samples 8-2a and 8-2b were found to experience shading effects due to the adjacent sample bottle 8-1a and 8-1b. Even though, the samples were left longer to grow in the proposed light condition, the cells did not perform stable lipid growth. Normally, when cells are under insufficient light, they become photolimited which affects

the growth rate and the other physiology of microalgal cells. Later when light was provided, the cell division should have improved but it did not. It could be because the light condition was not sufficient for lipid accumulation. This finding further highlights the effects of light intensity and photoperiod for enhanced lipid accumulation at stationary phase. Furthermore, the lipid growth in both the graphs excluding the sample 8-2 case, seemed to saturate at late stationary phase as seen from the last three stable values however, no conclusions can be made if the lipid growth further saturates or still increases after the stationary phase. In further experiment, it would be interesting to examine the changes in lipid content at late stationary phase for *P. tricornutum*.

7.8 Lipid Growth model and validation

Lipid growth model was made using the NR per DW as a function of Irradiance (I), day length (L) and time (t) in this experiment. The value from NR per DW is used as response variable in the design matrix. The design variables used in this model are shown in Table 6. The main constraints in this design were different sampling days for the photoperiod 8 and 20 h. If the effect per day were to be studied, the design condition has to be the same throughout the course.

As mentioned previously, the model summary of NR per DW with respect to t_1 did not show significant effects neither independently nor with the combination day photoperiod (L) and irradiance (I). This means, the effects of photoperiods and irradiance on lipid accumulation were not seen significant at the exponential phase. The R summary output for Model 2 corresponding to time t_2 at stationary phase, however, gave a very good response of lipids numbers with respect to irradiance and day length. The contour plot of Model 2 showed a very well fit with the observed data. In addition, it also showed the changes in lipid content at low light and high light conditions. The differences seen were very significant and can be explained by the physiological change that occurs in the photosynthetic apparatus when moving from dark cycle to light cycle. During the dark cycle, respiration losses and cellular metabolism is more common.

Brown et. al (1996) studied the effect of dark light cycle and irradiance on some cellular components like carbohydrates, proteins and lipids in algae *Thalassiosira pseudonana*. Three different forms of treatments were used: $50 \mu\text{mol}\cdot\text{photons}\cdot\text{m}^{-2}\cdot\text{s}^{-1}$ in day length of 24 h, $100 \mu\text{mol}\cdot\text{photons}\cdot\text{m}^{-2}\cdot\text{s}^{-1}$ in 12 h and $100 \mu\text{mol}\cdot\text{photons}\cdot\text{m}^{-2}\cdot\text{s}^{-1}$ in 24 h lights.

Main findings in this study were that the longer the photoperiod, the higher is the growth rate and vice-versa. In addition, the lipid content as a percentage of dry weight also did not seem to be affected by day length during the exponential phase. Similarly, the values of NR per DW at exponential phase in this study also showed no increase or decrease in lipid content at the exponential phase. Moreover, the study by Brown et.al (1996) also observed lower values of lipids at lowest irradiance in exponential phase. The findings by Brown et al (1996) somewhat seem to resemble with the results of this study showing the lowest lipids number at the lowest irradiance at stationary phase growth.

Similar studies done for other microalgae species have found the effects to be similar as in this study. A study by Richardson et.al (1983) reported microalgae cultivated at various light intensities and light regimes exhibited remarkable changes in their gross chemical composition, pigment content and photosynthetic activity. Another report by Harwood (1998) suggested that the dark-light regimes and different light intensities bring remarkable changes by altering the lipid profile. This supports the difference in NR per DW results obtained at different light regimes in the model above in Figure 26. Often, cells when moving from shorter day length to longer day length seem to have bigger effects on the chemical composition or pigments which can alter the metabolism and hence, the lipid content. Additionally, Khotimchenko and Yakovleva (2005) also highlighted the importance of light that normally stimulates the fatty acid synthesis, growth and formation of (particularly chloroplast) membranes. Cultures grown at strong irradiance and longer day light regime are found to have higher amount of triacylglycerides with saturated and mono saturated fatty acids compared to the ones at less light and the differences can be seen in such morphological changes Wahdin et.al (2012).

On the basis of the overall scientific reviews and the results obtained from this experiment, it can be said that the light irradiance and the photoperiod have significant effects on the lipid accumulation in microalgae *P. tricornutum* at stationary phase. In other words, the lipid content value varies remarkably from exponential phase growth to the stationary phase due to nutrient limitation and metabolic alteration. And this variation is strongly affected by the light irradiance and the photoperiod.

8 Conclusions

The first goal of the study was to quantify the effects of the photoperiod and the irradiances on the growth and lipid content in the microalgae *P. tricornutum*. The experiment was arranged at four fixed irradiance levels 400, 180, 40, 20 $\mu\text{mol}\cdot\text{q}\cdot\text{m}^{-2}\cdot\text{s}^{-1}$ with six different light periods 4,8,12,16,20,24 h under LED light panel. The species *P. tricornutum* was cultivated in nutrient-replete media under controlled laboratory conditions. The results showed that it is not only the irradiance levels but also the light exposure hours that affect the growth rates of microalgae *P. tricornutum*. A phenomenon of photo inhibition was also observed at higher photoperiod, i.e. 24 h. Similarly, the Chla per dry weight measurement showed general decreasing trend of Chla per dry weight when moving from lower light doses to higher light doses; however the data also contained some noise. To make specific conclusions on chlorophyll synthesis mechanics of microalgae *P. tricornutum* would still require further experiments. Moreover, the NR fluorescence per dry weight data showed a linear relationship in lipid accumulation at longer photoperiods. The maximum lipid accumulation was found at high irradiance condition, however, no significant trend was observed on the lipid accumulation at varying photoperiods at the exponential phase. Hence, to study the lipid accumulation the second experiment was designed at the stationary phase in nutrient limited media.

The second aim of the experiment was to quantify the effects of light irradiance and photoperiods on the total lipid content at the stationary phase. Two light levels: higher i.e. 180 $\mu\text{mol}\cdot\text{q}\cdot\text{m}^{-2}\cdot\text{s}^{-1}$ and lower i.e. 72 $\mu\text{mol}\cdot\text{q}\cdot\text{m}^{-2}\cdot\text{s}^{-1}$ at photoperiod of 20 h and 8 h were chosen for the study. The species *P. tricornutum* were cultivated under nutrient-deplete conditions. The results showed that the maximum lipid accumulation at the irradiance of 180 $\mu\text{mol}\cdot\text{q}\cdot\text{m}^{-2}\cdot\text{s}^{-1}$ at longer photoperiod 20 h and the minimum at irradiance of 72 $\mu\text{mol}\cdot\text{q}\cdot\text{m}^{-2}\cdot\text{s}^{-1}$ at photoperiod 8 h. The variation due to lowest light condition could not be fully understood, due to self-shading problems which are more common in experimental arrangements as such. Moreover, it was also tricky to determine the actual sampling points. A lipid variation model was also made in R in order to see if the effects of the photoperiod and the irradiance were statistically significant. The effects of light irradiance and photoperiod on lipid content were seen significant only at the stationary phase.

The overall aim was to assess and quantify the effects of light irradiance and photoperiod on the algal growth and the lipid content and also to understand the production lim-

its in larger scale microalgae cultivation globally. Although, the global irradiance map showed that most parts of the globe favors the cultivation of microalgae, only the areas with low variation in temperature and seasonal changes are suitable to maintain a year-round productivity. Hence, the start up the commercial scale microalgae cultivation units is not that easy. As pointed out from the results in this thesis, light intensity and photoperiod has significant effects on the growth rate and lipid content in microalgae *P.tricornutum* .There are also several other factors such as nutrients, temperature, pH, salinity etc that affects the productivity. Thus, those factors have to be studied and optimized prior to the scale up cultivation plan. Furthermore, the technical aspects regarding the commercial production of microalgae has to be understood and the natural phenomenon such as photoinhibition, photosaturation, evaporation losses and self-shading in the cultivation units has to be minimized.

In future experiments, it would be very interesting to assess the increase or decrease in lipid content of *P. tricornutum* at the late stationary phase. By doing so, it will be easier to examine and optimize the exact sampling point for lipid harvesting to get the maximum productivity in larger-scale microalgae cultivation. Furthermore, limitations such as self-shadings can be avoided in future experiments. In addition, measurements such as LC₁, LC₂, OJIP, and NPQ were carried using aqua pen and chlorophyll spectra measurements were made using spectrophotometer in this experiment. Those results are not discussed in this thesis because it is beyond the scope of this thesis topic.

In summary, microalgae stand out as an ideal biofuel solution to the increasing fuel crisis and could also be an ideal replacement to the fossil fuels. However, for algae fuel to fully emerge as a commercial biofuel, still requires various research in the field of microalgae genetics, growth kinetics, photobiology and understanding of economical and technical aspects related to cultivation and harvesting units.

References

1. Beardall,J.,Johnston,A.Mand Raven ,J.A (1998) environmental regulation of CO₂ concentrating mechanism in cyanobacteria and microalge.Canadian Journal of Botany.76:1010-1017
2. Beardall,J.,Joung,E.and Roberts,S.(2001) approaches for determining phytoplankton nutrient limitation. Aquatic Science.63:44-69
3. Bonente, G., Formighieri, C., Mantelli, M., Catalanotti, C., Giuliano, G., Morosinotto, T., Bassi, R. (2011) Mutagenesis and phenotypic selection as a strategy toward domestication of *Chlamydomonas reinhardtii* strains for improved performance in photobioreactors, *Photosynthetic Research*, 208: 107-120
4. BP statistical Review of World Energy June 2013, www.bp.com/statisticalreview retrieved on 12.04.2014.
5. Brennan L, Owende P. biofuels from microalgae- a review of technologies for production, processing and extraction of biofuels and co-products. *Renew Sustain Energy Rev* (2009).dpo:10.1016/j.rsr.2009.10.009.
6. Brand,L.E.(1994)Physiological ecology of marine coccolithophores.In: coccolithophores.(winter,A and Seisser,W.G.eds). Cambridge University Press,Cambridge,pp:39-49
7. Buitenhuis,E.T,de Baar,H.J.W and Veldhuis ,M.J.W.(1999)Photosynthesis and calcification by *Emiliana Huxley* (Prymnesiophyceae) as function of inorganic carbon species.*Journal of Phycology*.35:949-959
8. Chisti Y, Research reviewpaper: Biodiesel from microalgae, 2007Institute of technology and Engineering, Massey University, *Biotechnolgy Advances* 25,294-306.

9. Collet, P., Hélias, A., Lardon, L., Ras, M., Goy, R-A., Steyer, J-P. (2011) Life-cycle assessment of microalgae culture coupled to biogas production, *Bioresource Technology*, 102:207-214
10. Darzins A, Pienkos P, Edye L (2010), Current status and potential for algal bio-fuels production. A report to IEA Bioenergy task 39; Report T39T2, 131 pp.]
11. Droop,M.R.(1973) Some thoughts on the limitation in algae. *Journal of Phycology*:9:264-272
12. Falkoski, P. G and Raven, J. A, *Aquatic photosynthesis*, Blackwell Science USA 1997, 375p.
13. Fogg and Thake et. al, *Algal cultures and Phytoplankton Ecology*, The University of Wisconsin Press, 1987, Science (3-95).
14. Global Irradiance Map Meteotest; database Meteonorm (www.meteonorm.com)
15. Halim.R., Danquah M.Webley.P.A,Extraction of oil from microalgae for biodiesel production: A review, *Biotechnology advances* 30(2012) 709-732.
16. Hardwood, J.L, 1998.Membrane lipids in algae. In: Siegenthaler, P.A, Murata,N.(Eds.),*Lipids in photosynthesis: Structure,Function and Genetics*.Kluwer Academic Publishers.,Kluwer,Netherlands.
17. Huge. L. MacIntyre, Todd. M Kana 2002, Photo acclimation of photosynthesis irradiance response curves and photosynthetic pigments in microalgae and cyanobacteria, University of Maryland Centre for Environmental Science, Cambridge, USA.
18. International Energy Agency, *World Energy Statistics 2013*,
<http://www.iea.org/publications/freepublications/publication/KeyWorld2013.pdf>
on 2.5.2014.
19. Janssen M, *Cultivation of microalgae: Effect of light /dark cycles on biomass yield*, Thesis,Wageningen University,Wageningen, The Netherlands, 2002,

20. J. Pruvost, G. Van Vooren, G. Cogne, J. Legrand, Investigation of biomass and lipids production with *Neochloris oleoabundans* in photobioreactors, *Bioresource Technology* 100 (2009) 5988–5995.
21. Kates M. Definition and classification of lipids. *Techniques of lipidology isolation, analysis, and identification of lipids*. Amsterdam: Elsevier Science Publisher; 1986a.
22. Kates M. Lipid extraction procedures. *Techniques of lipidology isolation, analysis, and identification of lipids*. Amsterdam: Elsevier Science Publisher; 1986b.
23. Khotimchenko, S.V., Yakovelva, I.M., 2005 Lipid composition of red alga *Tichocarpus crinitus* exposed to different levels of photon irradiance. *Phytochemistry* 66, 73-79.
24. Khosla V. Where will biofuels and biomass feedstocks come from? [White Paper], Available from: <http://www.khoslaadventures.com/presentations/WherewillBiomasscomeFrom.doc>[aa.06.08];2009.p.31.
25. Knothe G, Dunn RO, Bagby MO. Biodiesel: the use of vegetable oils and their derivatives as alternative diesel fuels. *ACS Symp Ser* 1997; 666:172 208.
26. Knothe G. Analyzing biodiesel: standards and other methods. *J Am Oil Chem Soc* 2006; 83:823–33.
27. Lang X, Dalai AK, Bakhshi NN, Reaney MJ, Hertz PB. Preparation and characterization of bio-diesels from various bio-oils. *Bioresource Technology* 2001; 80:53–62.
28. Lage, O.M, Darente, A.M, Soares, H.M.V.M, Vasconcelos, M.T.S D and Salen, R. (1994) some effects of copper on the dinoflagellates *Amphidinium carterae* and *Prorocentrum micans* in batch culture. *European Journal of Phycology*. 29:253-260.

29. Langdon.C.on the causes of interspecific differences in the growth irradiance relationship for phytoplankton.II. A general review, Graduate school of Oceanography, University of Rhode Island. Journal of phytoplankton research Vol. No 1291-1312, 1988.
30. L. Rodolfi, G.C. Zittelli, N. Bassi, G. Padovani, N. Biondi, G. Bonini, M.R. Tredici, Microalgae for oil: strain selection, induction of lipid synthesis and outdoor masscultivation in a low-cost photobioreactor, *Biotechnology and Bioengineering* 102(2009) 100–112.
31. Maddux,W.S and Jones R.F (1964) some interactions of temperature, light intensity and nutrient concentration during the continuous culture of *Nitzschia closterium* and *Tetraselmis* sp. *Limnology and Oceanography*.9:79-86
32. Meng X. Yang J, Xu X Zhang L, Nie Q Xian M. Biodiesel production from oleaginous microorganisms. *Renewable Energy* 2009; 34(1); 1-5.
33. Metting FB.Biodiversity and application of microalgae's *Ind Microbiology* 1996;17:477-89.
34. Metting B,Pyne JW.Biologically-active compounds from microalgae. *Enzyme Microb.Technology* 1986; 8:386-94.
35. Moore A. biofuels are dread:long live biofuels(+)-åart one .*New Biotechnology* 2088; 25(1);6-12.
36. Morel,F.M.M., Reinfelder,J.R.,s.B.,Chamberlain,C.P.,Lee,J.G and Yee,D(1994) Zinc and carbon co-limitation of marine phytoplankton. *Nature*.396:740-742
37. Moo-Young, M, Chisti .Y,Considerations for designing bioreactors for shear-sensitive culture .*Biotechnology* 1988; 6; 1291-6.
38. Natunen K, Quantification of Neutral lipids in phytoplankton cultures with the Nile Red method, Master's thesis, Aalto University,Espoo, 2012.

39. Nagle N, Lemke P. Production of methyl-ester fuel from microalgae. *Appl Biochem Biotechnol* 1990;24–5:355–61.
40. Necton report (1990) Estudo de localização de unidade industrial para produção de microalgas em portugal. 71 pp]
41. Oliver.G.J, Muntean.M, 2013, Trends in global CO2 emissions: 2013 Report. Netherlands Environmental Assessment Agency.ISBN 978-94-91506-51-2.
42. Pandey, Lee and Chisti et.al.Biofuels from Algae 2013, ISBN: 978-0-444-59558-4, Methods of algae harvesting Chapter 5.
43. Parmar, A., Singh, N.K., Pandey, A., Gnansounou, E., Madamwar, D. (2011) Cyanobacteria and microalgae: a positive prospect for biofuels, *Bioresource Technology*, 102: 10163-10172
44. Park, J.B.K., Craggs, R.J., Shilton, A.N. (2011) Recycling algae to improve species control and harvest efficiency from a high rate algal pond, *Water Research*, 45: 6637-664.
45. Posthuma M. A, Microalgae Biofuel production, Options for process optimization and Environmental assessment of Resources. Energy balances and CO2 emissions. Master's thesis. Universiteit Utrecht .The Netherlands.2009
46. Q. Hu, M. Sommerfeld, E. Jarvis, M.L. Ghirardi, M. Posewitz, M. Seibert, A. Darzins, Microalgal triacylglycerols as feedstocks for biofuels production: perspectives and advances, *The Plant Journal* 54 (2008) 621–639.
47. Report on Biology and Biotechnology of algae with indication of criteria for strain selection; Algae and aquatic biomass for sustainable production of 2nd generation biofuels. Retrieved on 22 .04.2014
http://www.aquafuels.eu/attachments/079_D%201.4%20Biology%20Biotechnology.pdf
48. Reynolds, C., *Ecology of Phytoplankton*, Cambridge University Press, USA 2006, 535 p.

49. Rhee, G., Y and Gotham, I. J. (1981) The effect of environmental factors on phytoplankton growth: temperature and the interactions of temperature with nutrient limitation. *Limnology and Oceanography* 26:635-648.
50. Richmond, A and Zou, N. (1999) Efficient utilization of high photon irradiance for mass production of photoautotrophic micro-organisms. *Journal of Applied Phycology*. 11:123-127
51. Richmond, A (1987) The challenge confronting industrial microagriculture: high photosynthetic efficiency in large-scale reactors. *Hydrobiologia* 151/152:117-121
52. Richmond, A (1988) *Spirulina*. In: *Microalgal biotechnology*. (Borowitzka, M. A and Borowitzka, L. J. eds). Cambridge University Press, Cambridge, pp:85-121
53. Richardson, K., Beardall, J., Raven J. A 1983 Adaptation of unicellular algae to irradiance. An analysis of strategies. *New Phytol.* 93, 1957-191.
54. Robert Arthur Anderson, 2005, *Algal culturing techniques* ISBN:0-12-088426-7 , page 305
55. Samuel I. Beale, David Appleman, 1987, Chlorophyll synthesis in *Chlorella*: Regulation by Degree of light limitation of growth; *Plant Physiology* February; 47(2): 230-235.
56. Schwenk, D., Seppälä, J., Spilling, K., Virkki, A., Tamminen, T., Oksman-Caldentey, K.-M., Rischer, H. (2013) Lipid content in 19 brackish and marine microalgae: influence of growth phase, salinity and temperature. *Aquatic Ecology*, 47:415-424.
57. Singh, A., Nigam, P. S., Murphy, J. D (2011a) Renewable fuels from algae: an answer to debatable land-based fuels, *Bioresour. Technol.* 102:10-16.
58. Smith, H. D. (2012), PhD thesis. Microalgae for biochemical conversion of CO₂ and production of Biodiesel, University of Bath, Department of Biology and Biochemistry.

59. Seppälä, J. (ed.) 2013: Potential uses of micro-macro algae in the Baltic Sea Region SUBMARINER Report 10/2013.
60. Spilling, K., Seppälä, J. (2012) Photobiology and lipid metabolism in algae. In Gordon R. and Seckbach J. (Eds.) the science of algal fuels: phycology, geology, biophotonics, genomics and nanotechnology. Dordrecht, Springer, pp 385-398.
61. Taylor, F.J.R. (1987) Ecology of dinoflagellates; general and marine ecosystems. In: The Biology of Dinoflagellates. (Taylor, F.J.R. ed), Vol 21. Blackwell Scientific Publications, Oxford, pp: 389-502
62. Teresa, M.M., Antonio A. M., Nidia S. Caetano (2009), Microalgae for biodiesel production and other applications: A review, Renewable and Sustainable Energy Reviews 14 (2010) 217-232.
63. Tredici, M.R. (2010) Photobiology of microalgae mass cultures: understanding the tools for the next green revolution. Biofuels 1: 143–162.
64. Tredici, M.R. (2004) Mass Production of microalgae: Photo bioreactors. In: Richmond A. (ed.) Handbook of Microalgal culture. Blackwell Science Ltd, Oxford pp 178-214.
65. Tredici, M.R., Chini, Zittelli, G., Rodolfi, L. (2010) Photo bioreactors In: Flickinger M.C., Anderson S. (eds) Encyclopedia of Industrial Biotechnology: Bio process, Bio separation and Cell Technology. John Wiley and Sons, Inc., Hoboken, NJ, USA Vol 6. pp. 3821-3838.
66. Wahidin S., Idris, A., Shaleh, Muhamad R.S. (2012) The influence of light intensity and photoperiod on lipid content of microalgae *Nannochloropsis* sp. Bioresource tech 129(2013) 7-11.
67. Wang B., Li Y., Wu N., Lan C., CO₂ bio-mitigation using microalgae. Applied Microbiology and Biotechnology 2008; 79(5): 707-18.

68. Ugwu CU, Aoyagi H, Uchiyama H Photobioreactors for mass cultivation of algae. *Bioresource Technology* 2008;99(10):4021-8.

69. Picture 1 <http://classroom.sdmesa.edu/eschmid/Lecture11-Microbio.htm>

T-2 Media Composition

T-2 (Kristian Spilling 14.3.2006)			
The macronutrients are adjusted to the molar ratios: N: P = 16. N: Si = 2.			
Trace metal solution is the same as in the L-1 media (Guillard and Hargraves 1993) and vitamins as the f/2 media (Guillard and Ryther 1963. Guillard 1975).			
Stock 1-4 is to be stored in a refrigerator (4°C), stock 5 (vitamins) is to be stored in a deep freezer (-20°C)			
T-2 MEDIA			
Into 1 L of filtered. Autoclaved sea water			
Stock 1 (N)	1 ml	Final concentration	
Stock 2 (P)	1 ml	580 µmol L-1 (8.12 mg L-1)	
Stock 3 (Si)	0.5 ml	36.3 µmol L-1 (1.13 mg L-1)	
Stock 4 (METALS)	1 ml	290 µmol L-1 (8.14 mg L-1)	
Stock 5 (VITAMINS)	1 ml	see below	
		see below	
Making stock solutions			
Macronutrients	Chemical	Added	Stock volume
Stock 1 (N)	NaNO3	4.930 g (580 mM)	100 ml
Stock 2 (P)	K2HPO4	0.632 g (36.3 mM)	100 ml
Stock 3 (Si)	Na2SiO39H2O	8.242 g (290 mM)	100 ml
Micronutrients			
For stock 4:			
Primary trace metals			
	CuSO4 5H2O	0.250 g	
	ZnSO4 7H2O	2.200 g	
	CoCl2 6H2O	1.000 g	
	MnCl2 4H2O	18.000 g	
	NaMoO4 2H2O	1.890 g	
	H2SeO3	0.130 g	
	K2CrO4	0.194 g	
	Na3VO4	0.184 g	
	NiSO4 4H2O	0.270 g	
Added to 100 ml Milli-Q			
Chemical			
		Added	Stock volume
Stock 4 (Metals)	Na2EDTA	0.436 g	100 ml
	FeCl3 6H2O	0.315 g	
	Primary trace metal solution	0.100 ml	
Added to 100 ml Milli-Q			
For stock 5:			
Primary vitamins	Biotin	0.001 g	
	B12	0.010 g	
Each added to 10 ml Milli-Q separately			Stock volume
Stock 5 (Vitamins)	Dissolved Biotin	0.500 ml	100 ml
	Dissolved B12	0.050 ml	
	Thiamine HCl (B1)	0.010 g	
Added to 100 ml Milli-Q			
FINAL MEDIA: ALL STOCKS ARE ADDED 1ML TO 1000 ML OF AUTOCLAVED WATER			
Final concentration of	Metals:		
Vitamins:	CuSO4 5H2O = 0.0250 µg L-1		
Biotin = 0.5 ng L-1	ZnSO4 7H2O = 0.2200 µg L-1		
B12 = 0.5 ng L-1	CoCl2 6H2O = 0.1000 µg L-1		
Thiamine = 1 ng L-1	MnCl2 4H2O= 1.8000 µg L-1		
	NaMoO4 2H2O = 0.1890 µg L-1		
	H2SeO3 = 0.0130 µg L-1		
	K2CrO4 = 0.0194 µg L-1		
	Na3VO4 = 0.0184 µg L-1		
	NiSO4 4H2O = 0.0270 µg L-1		
	Na2EDTA = 436 µg L-1		
	FeCl3 6H2O = 315 µg L-1		